

RESEARCH

Open Access



# Incorporation of kiwifruit peel improved the property of carboxymethyl cellulose-gum Arabic active film and its effects on the quality of beef sausages

Evans Frimpong Boateng<sup>1</sup>, Ziyi Yang<sup>1</sup>, Jian Zhang<sup>1</sup>, Lei Zhou<sup>1</sup>, Lujuan Xing<sup>1</sup> and Wangang Zhang<sup>1\*</sup>

## Abstract

In the present study, different doses of lyophilized kiwifruit peel powder extract (KPE) were incorporated into carboxymethyl cellulose (CMC) and gum Arabic (GA) based polymer matrices to fabricate films CG-CT (control film), CG-KPE1 (1% KPE), CG-KPE2 (2% KPE), and CG-KPE3 (3% KPE) to investigate their effects on active packaging functionality and sliced-beef sausage quality. Consequently, CG-KPE films demonstrated a superior antimicrobial effect on Gram-positive (*Staphylococcus aureus* and *Bacillus cereus*) and Gram-negative (*Escherichia coli*) bacteria and antioxidant efficacy compared to CG-CT films. The scanning electronic microscopy (SEM) of CG-KPE films revealed an enhanced micrograph. Fourier transform infrared spectroscopy (FTIR) and differential scanning calorimetry (DSC) evidenced the intramolecular interaction between KPE and CG and the improved thermal stability of film matrix. Film X-ray diffraction (XRD) peaks revealed a good crystallinity. CG-KPE films exhibited better physical and mechanical properties, increased opacity, and better ultraviolet (UV) emission barrier due to KPE addition and pigmentation compared to CG-CT films. The quick biodegradability of CG-KPE film suggested potential for KPE as a biopolymer. Subsequently, sliced-beef sausages were packaged with CG-CT, CG-KPE1, CG-KPE2, and CG-KPE3 (respective to CT, T1, T2, and T3) and stored for 12 d ( $4 \pm 1$  °C). The product's pH and moisture content were controlled due to KPE addition in CG-KPE films. The products revealed that during storage CG-KPE treatments had a positive impact on the textural property, the color stability, and the sensory quality compared to CG-CT treatments. CG-KPE treatments showed antimicrobial effectiveness and lesser TBARS values than CG-CT treatments during storage.

## Highlights

- KPE valorization as a biopolymer in a newly developed active film was studied.
- KPE films exhibited effective active packaging functionalities and biodegradability.
- Applications of fabricated active films in packaging sliced-beef sausages was effective.
- KPE film's enhanced sliced-beef sausages quality and shelf-life extension during storage.

**Keywords** Active packaging, Kiwifruit peel, Antioxidant, Antimicrobial, Biodegradability

\*Correspondence:

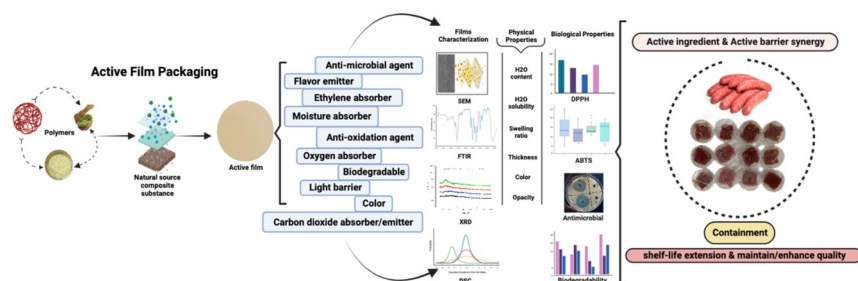
Wangang Zhang  
wangang.zhang@njau.edu.cn

Full list of author information is available at the end of the article



© The Author(s) 2025. **Open Access** This article is licensed under a Creative Commons Attribution 4.0 International License, which permits use, sharing, adaptation, distribution and reproduction in any medium or format, as long as you give appropriate credit to the original author(s) and the source, provide a link to the Creative Commons licence, and indicate if changes were made. The images or other third party material in this article are included in the article's Creative Commons licence, unless indicated otherwise in a credit line to the material. If material is not included in the article's Creative Commons licence and your intended use is not permitted by statutory regulation or exceeds the permitted use, you will need to obtain permission directly from the copyright holder. To view a copy of this licence, visit <http://creativecommons.org/licenses/by/4.0/>.

## Graphical Abstract



## Introduction

Beef sausages provide protein, minerals, vitamins, and essential micronutrients in the diets of consumers. However, they are perishable due to alteration caused by microbial spoilage and lipid oxidation, thus resulting in product quality loss and shelf-life reduction (Zhang et al., 2010). Packaging material prevents oxygen attack and chemical contamination, inhibits deterioration, exerts enzyme activity to enhance tenderness, prevents ultraviolet (UV) light, and controls the color, aroma, and weight losses of processed meat products (Pereira de Abreu et al., 2012). Successful studies of packaged meat products include beef muscle (Fu et al., 2017), chicken balls, chicken and mutton seekh kebabs (Kanatt et al., 2013), and pork sausages (Siripatrawan & Noipha, 2012). To a large extent, synthetic polymer utilization in packaging materials provides desirable features (transparency, softness, and lightness). However, these packaging materials are associated with environmental issues due to non-biodegradable synthetic polymers (Qin et al., 2020).

Active package functionality solely acts on the food to extend shelf-life and maintain nutritional quality (Drago et al., 2020). Carboxymethyl cellulose (CMC) is a linear biopolymer composed of several carboxyl groups with dominant coordination efficacy with metal cations ( $\text{Fe}^{3+}$ ) for hydrogel bead formation (Ghawanmeh et al., 2024). A reaction of sodium monochloroacetate with cellulose in an alkaline medium result in CMC (da Costa et al., 2023). CMC is soluble in water with a polyelectrolyte property, which could be utilized as viscosity modifier. As an ionic modified cellulose derivative, CMC is odorless and tasteless white powder highly soluble in alkaline solutions or water (Salehi et al., 2023; Tyagi & Thakur, 2023). CMC is utilized as a bioactive polymer in film development, possessing properties of high biocompatibility, no toxicity, excellent biodegradability, abundant presence, and acceptable production

cost. However, a few drawbacks associated with pure CMC include low flexibility, gel fraction, mechanical strength, and thermal stability. Therefore, a combination with other polymer's synergetic effect in the packaging industry has invaded the food industry with robust outcomes. Kuchaiyaphum et al. (2024) reported the extension of fresh pork shelf life by CMC/polyvinyl alcohol (PVA) doped with tamarind seed coat waste extract active packaging films. Also, a highly stretchable and versatile sodium CMC/PVA/poly ethylene imine/tannic acid hydrogel film revealed an efficient food packaging and preservation system by extending the shelf life of fresh mangoes, cherries, and strawberries (Zhao et al., 2022).

Gum Arabic (GA) is the exudate from Acacia species (*Acacia senegal* and *Acacia seyal*) branches and stems, which has a multi-branched complex molecular structure dominated by arabinogalactin with a natural hydrocolloid's properties. GA is either neutral or slightly acidic and consists of calcium, potassium, and magnesium salt. As the oldest natural and industrially used gum, glucuronic acid, rhamnose, glycoprotein, monosaccharides, oligosaccharides, arabinogalactans, and arabinose are among the chemical composition of GA polysaccharide-based polymers (Kang et al., 2021a; Tiamiyu et al., 2023). GA is nontoxic as a renewable source material in many applications in food, biosensors, tissue engineering, and drug delivery (Venkatesan et al., 2023). In the quest for functional and ecological friendly packaging materials, GA has been utilized in GA-based films in packaging pomegranate (*Punica granatum* L., cv. Wonderful) (Khedr, 2022), walnut kernel (Ebrahimzadeh et al., 2019), sunflower oil (Alnadari et al., 2022), eggs (Sariyel et al., 2022), and chicken and beef (Alnadari et al., 2023a). In addition, biopolymer GA has a strong hydrophilicity property and is utilized as a thickener and emulsifier in film development (Kang et al., 2021a).

China continues to be the world's leading kiwifruit producer with multiple and diverse cultivars grown across the following provinces:—Shaanxi, Gansu, Henan, Guangdong, Guangxi, Fujian, Guizhou, Yunnan, and Sichuan and areas of the Yangtze River basin (Yiling city in the Hubei province). Kiwifruit peel (KP) is hugely discarded yearly in the fruit industry due to the approximate 1 million metric tonnes of kiwifruits annually produced in the world (He et al., 2019; Ma et al., 2019). KP is an agricultural by-product, which is economically accessible and rich in antioxidant and antimicrobial content for valorization in the food industry. Solid-state fermentation, alcohol and citric acid production utilizes KP widely. Besides, KP could be used to produce the cysteine protease actinidin, an enzyme applied in meat tenderization or protein hydrolysis processes in the food industries (Sims & Monro, 2013).

Lyophilized kiwifruit peel powder extract (KPE) has the potential to compensate for synthetic antioxidant use in the food industry (Boateng et al., 2022; Wojdyło et al., 2017). However, there is no published study on KPE as a composite ingredient in producing active film for food packaging purposes.

Therefore, the current study aimed to incorporate KPE into CMC–GA composite matrix and develop an active packaging film. Further, the thermal, structural, morphology, physical characteristics, antioxidative, antimicrobial, and biodegradation functionalities of developed films were investigated. Lastly, the fabricated CG-KPE active films were used to package sliced-beef sausages to evaluate quality and safety indices during refrigerated storage.

## Materials and methods

### Materials

The entire study was carried out in the pilot plant and laboratory of the National Center of Meat Quality and Safety Control, Nanjing Agricultural University (Nanjing, Jiangsu, China). Physiologically matured kiwifruits (*Actinidia deliciosa* cv. Hayward) were sourced from an orchard in Zhouzi county (Shaanxi Province, China) located at 108° 3' 50" East longitude and 34° 17' 2" North latitude. Boneless round beef of 24 h *post mortem* cut and associated fat were purchased from a supermarket (Suguo Supermarket, Nanjing, China), and the pilot plant supplied seasonings for beef sausage formulations. Chemical and reagents included sodium CMC (Shanghai Macklin Biochemical, Shanghai, China), GA (Shanghai Yuanye Biological Technology, Shanghai, China), and glycerol (Solarbio Science and Technology, Beijing, China). 2,2-Diphenyl-1-picrylhydrazyl (DPPH) and 2,2'-azino-bis-(3-ethylbenzothiazoline-6-sulphonic acid) (ABTS) (Sigma, St. Louis, MO, USA). 2-Thio-barbituric acid (TBA), trichloroacetic acid (TCA), and plate count agar (PCA) (Sinopharm Chemical Reagent, Beijing,

China). Cephalothin-sodium fusidate-cetrimide (CFC) agar and streptomycin thallos acetate actidione (STAA) (Luqiao, Beijing, China), culture medium supplement (Qingdao Hope Bio-Technology, Qingdao, China), and all other chemicals used were of analytical grade. Scheme 1.

### Experimental plan

The experiment was conducted in two phases. The first phase comprised KPE incorporation in CMC–GA for active film development for physicochemical characterization, biodegradation test, and functional properties studies denoted as CG-CT (control), CG-KPE1 (1% KPE), CG-KPE2 (2% KPE), and CG-KPE3 (3% KPE). While in the second phase, sliced-beef sausages were packaged as CT, T1, T2, and T3 (denoted respectively to CG-CT, CG-KPE1, CG-KPE2, and CG-KPE3 developed films) for quality and safety synergetic assessment.

### Production of lyophilized kiwifruit peel extract (KPE)

The instrument (Christ Lyo Chamber Guard 121,550 PMMA, Beijing BMH Instrument, Beijing, China) at -80 °C for 72 h was used for lyophilized KPE production based on our previous study (Boateng et al., 2022).

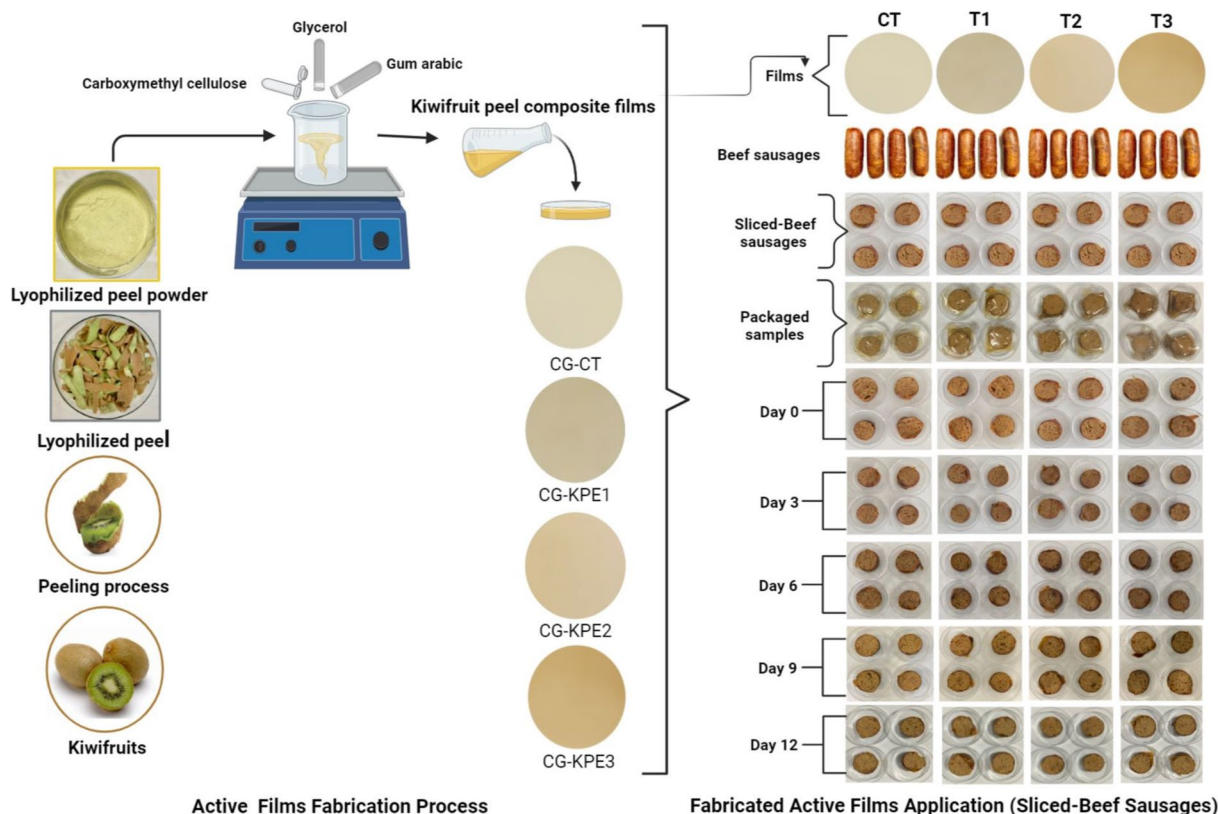
### Film preparation and production

The modified method outlined by Alnadari et al. (2023b) was employed for CG-KPE composite film preparation and production. The films were fabricated by dispersing CMC (6.0 g) and GA (2.0 g) in distilled water (400 mL). Next, the mixture was stirred (800 rpm) periodically at 60 °C for 2 h to dissolve. To achieve a plasticizer, the glycerol solution (35% w/w) based on CMC–GA weight was included. The mixture was stirred (800 rpm) at 50 °C for 30 min) thoroughly for homogeneity. Thereafter, KPE was incorporated at 0, 1, 2 and 3% concentrations based on CMC–GA content to secure treatments of CG-CT (control), CG-KPE1, CG-KPE2, and CG-KPE3, respectively. Each treatment was subjected to 800 rpm stirring at 40 °C for 1 h at pH 5 for a successive uniform mixture. Subsequently, 50 mL aliquot from individual treatment was poured into petri-dish plates (150 mm in diameter) and oven-dried (50 °C, 8 h). The produced films were then peeled off from the petri-dish plates and kept in a desiccator (30 °C) until later examination.

### Film antioxidant determination

The scavenging technique by Alnadari et al. (2023a) with slight modifications was utilized to evaluate antioxidant properties of films. DPPH and ABTS were estimated based on the subsequent equations.

$$\text{DPPH radical scavenging activity (\%)} = 1 - \frac{A_1 - A_2}{A_0} \times 100 \quad (1)$$



**Scheme 1** Schematic illustration of fabricated active films and application in sliced-beef sausages packaging. Source: Authors own elaboration.

Where  $A_0$  represents DPPH initial absorbance,  $A_1$  represents DPPH solution with the sample absorbance, and  $A_2$  represents the sample with water or methanol absorbance.

$$\text{ABTS radical scavenging activity (\%)} = 1 - \frac{A_1 - A_2}{A_0} \times 100 \quad (2)$$

Where  $A_0$  represents initial ABTS<sup>+</sup> absorbance,  $A_1$  represents sample absorbance, and  $A_2$  represents sample PBS absorbance.

#### Film antimicrobial activity by assay

The method outlined by Riaz et al. (2020) was employed for film microbial inhibition ability against two gram-positive bacteria (*Bacillus cereus* and *Staphylococcus aureus*) and one gram-negative (*Escherichia coli*) bacteria. Briefly, the disc of films (diameter 12 mm) was prepared and placed on agar media plates previously seeded with the bacteria culture suspension of 0.1 mL of a final concentration of  $1.5\text{--}3.0 \times 10^5$  CFU/mL by diluting with 0.3 mM PBS (6.8). Later the disc of films was exposed under UV light for sterilization and subsequently placed into Petri dishes containing solid medium carefully and

subjected to incubation at 37 °C for 24 h. The inhibition zone was estimated using a sliding caliper.

#### Film mechanisms and characterization

##### Chromaticity and opacity

To estimate the opacity the modified method outlined by Alnadari et al. (2023a) was employed. A UV-722 spectrophotometer (Shanghai Jinghua Science and Technology Instruments, China) was used to estimate film opacity at 600 nm. The thickness of the slice bands (80 mm length  $\times$  45 mm width) was assessed based on the equation below.

$$\text{Opacity} = A/L \quad (3)$$

Where A represents absorbance value at 600 nm and L represents film thickness (mm).

The Minolta colorimeter (CR-40, Minolta, Osaka, Japan) with D65 illuminate, a 0.13 mm diameter viewing area, and 0° viewing angle was utilized for film color determination. Prior to color measurements, a white tile (mod CR-A43) was employed for calibration. The total color differences ( $\Delta E$ ), white (WI), and yellow (YI) indexes were calculated by utilizing the equation

below. Where  $L^*$  represents lightness,  $a^*$  represents redness, and  $b^*$  represents yellowness.

$$\Delta E = \left( (L_i^* - L^*)^2 + (a_i^* - a^*)^2 + (b_i^* - b^*)^2 \right)^{1/2} \quad (4)$$

$$YI = \frac{142.68 \times b^*}{L^*} \quad (5)$$

$$WI = 100 - \left( (100 - L^*)^2 + a^{*2} \right)^{1/2} + b^{*2} \quad (6)$$

#### Film thickness

A digital hand-held micrometer (Mitutoyo Absolute, Tester Sangyo, Osaka, Japan) was used to estimate the film's thickness according to the slightly modified method employed by Alnadari et al. (2023a). Briefly, film samples were cut into 10 × 80 mm rectangular strips by utilizing a precision double blade cutter before estimating the film thickness. The individual sample was assessed 10 times randomly at various levels, and the mean was calculated.

#### X-ray diffraction (XRD)

The crystal structure of the film samples (1 × 1 cm) was identified using a powder X-ray diffractometer (D8 Advance, Bruker, USA) equipped with Cu-K $\alpha$  radiation Alnadari et al. (2023b). The measurements were performed at diffraction angle range 2 $\theta$  between 5–80° ambient conditions. The scanning speed was 15.6°/min. Examination of the films was done at 30 kV and 10 mA.

#### Scanning electronic microscopy (SEM)

The modified technique outlined by Alnadari et al. (2022) was employed. SEM (SU8010, Hitachi, High Technologies, Tokyo, Japan) was employed at 10 kV to investigate the films' morphology. The films were cut in 10 × 10 mm dimensions and mounted on an aluminum stubby using double-sided carbon tape and a gold-covered sputter (MC 1000 Ion Sputter Coater, Hitachi High Technologies, Tokyo, Japan). The magnification was set at 3000×.

#### Differential scanning calorimetry (DSC)

The modified technique outlined by Alnadari et al. (2023b) was used. Briefly, 10 mg pieces of films were sealed in a standard aluminum pan which was heated under a nitrogen atmosphere from 32 to 450 °C at a rate of 10 °C/ min. DSC (DSC-60, Shimadzu, Kyoto, Japan) was used to analyze the film's thermal properties.

#### Film's mechanical characteristics

The texture instrument (TA.XT Plus, Stable Micro Systems, Surrey, UK) was used to analyze the fabricated film's mechanical features, including tensile strength (TS) and elongation break (EB), based on a modified protocol of Alnadari et al. (2022). The films were examined in triplicate. Subsequently, the equation below was employed to compute the means of EB and TS per the resistance values to extension (N) and extensibility (mm).

$$EB(\%) = \frac{\Delta L}{L} \times 100 \quad (7)$$

$$TS(\text{MPa}) = \frac{F}{X \times W} \times 100 \quad (8)$$

Where F represents resistance to extension (N), X represents thickness of film (mm), W represents film width (mm),  $\Delta L$  represents film increased distance at the break (mm) and L represents film (mm) original length between grips.

#### Fourier transform infrared spectroscopy (FTIR)

Nasiru et al. (2023) outlined FTIR techniques was employed. FTIR spectroscopy (Nicolet iS-150 FTIR-ATR, Thermo Fisher Scientific, MA, USA) with a 4000–400  $\text{cm}^{-1}$  frequency range with the resolution of 32 scans at 4  $\text{cm}^{-1}$  was employed to analyze the CMC, GA, and KPE powders (3 mg) and prepared film's initial structures.

#### Swelling ratio, moisture, and films solubility measurement

Alnadari et al. (2022) protocol was adopted for developed film swelling ratio, solubility, and moisture determination. Briefly 20 × 20 mm film bands were weighed as wet weight ( $M_0$ ) and dried at 105 °C to achieve a constant weight to calculate the primary dry mass value ( $M_1$ ). Further, the dried pieces were subjected to 100 mL beaker containing distilled water (50 mL) covered with plastic wraps and stored at 25 °C for 24 h. The film samples were again dehydrated superficially with filter papers and weighed to secure  $M_2$ . At 105 °C, the saturated-hydrate films were dehydrated to constant to obtain final dry mass  $M_3$ . Hence, the equations below were adopted to measure the film solubility, moisture amount, and swelling ratio parameters.

$$\text{Moisture content (\%)} = \frac{M_0 - M_1}{M_0} \times 100 \quad (9)$$

$$\text{Swelling ratio (\%)} = \frac{M_2 - M_0}{M_0} \times 100 \quad (10)$$

$$\text{Film solubility (\%)} = \frac{M_1 - M_3}{M_1} \times 100 \quad (11)$$

Where  $M_0$  represents film initial mass,  $M_1$  represents film initial dry-weight,  $M_2$  represents film mass after 24 h drenching in water, and  $M_3$  represents film dry mass after 24 h drenching in water.

#### Film biodegradation test

The composting test (soil burial test) reported by Tan et al. (2016) was adopted to determine the film's bio-disintegration capacity. Briefly, the College of Agriculture experimental field humus sample in Nanjing Agricultural University (Nanjing, China) was collected into a flower pot to serve as the study area. Each film sample (2 × 2 cm) was buried at a 4 cm depth for 21 d in a 65% moisture soil (10–25 °C). Daily, the soil was treated twice with water. The films were removed weekly to estimate their mass loss according to the equation below:

$$\text{Weight loss (\%)} = \frac{M_0 - M_1}{M_0} \times 100 \quad (12)$$

Where  $M_0$  represents film initial mass, and  $M_1$  represents film mass after 7, 14 and 21 d of biodegradation.

#### Sliced beef sausages manufacture and packaging

Four different groups of beef sausages were prepared based on a similar procedure of our previous study (Boateng et al., 2022) and sausage slices (1.5 × 1.5 cm), each containing the primary ingredient of mixed spices (1.20%), NaNO<sub>2</sub>/NaNO<sub>3</sub> (0.12%), garlic powder (0.80%), red pepper powder (0.50%), onion powder (1.20%), black pepper powder (0.50%), and cold water (9.00%). Further, the fabricated active films including CG-CT, CG-KPE1, CG-KPE2, and CG-KPE3 were used to package the sliced beef sausage corresponding to CT (control), T1, T2, and T3 experimental samples respectively and shelved at 4 ± 1 °C, ahead of later analysis. Each treatment was randomly selected for analysis at 0, 3, 6, 9 and 12 d.

#### pH

A modified pH method by Bassey et al. (2021) was employed. The desktop pH meter (FE-20, Mettler Toledo, Zurich, Switzerland) adjusted with buffer solution (pH 4, 7 and 10) was used to determine the pH value of packaged slices homogenate after 0, 3, 6, 9 and 12 d of refrigerated storage.

#### Color

A modified color method by Boateng et al. (2022) was employed. A portable colorimeter (Chroma Meter CR-400, Konica Minolta Sensing, Sakai, Japan) with illuminant (D 65), viewing area (0°), and viewing area diameter (0.13 mm) was used to attain the surface color of packaged slices after 0, 3, 6, 9 and 12 d of refrigerator storage. Each sample was assessed three times at different surface positions by measuring lightness ( $L^*$ ), redness ( $a^*$ ), and yellowness ( $b^*$ ). The mean values were used for the statistical analysis.

#### Texture profile determination

The TA. XT Plus with P50 probe (Stable Micro System, Surrey, UK) was used for texture profile analysis (TPA) of packaged slices by adopting the method outlined by Gao et al. (2014) with slight moderation after 0, 3, 6, 9 and 12 d of refrigerated preservation. The mean values of triplicated samples per each experimental treatment were used for analysis.

#### Electronic nose

The technique outlined by Zhang et al. (2020) was adopted with a slight modification to execute the e-nose analysis of the packaged beef sausage slices stored at 12 d.

#### Lipid oxidation determination

The TBARS were evaluated with a slight moderation upon the protocol of Zhang et al. (2021). TBARS values were expressed as mg malondialdehyde (MDA)/kg of meat sample. The samples were evaluated in triplicates.

#### Moisture content measurement

The moisture content of the packaged sliced-beef sausages stored at 12 d were determined using an electronic hygrometer analyzer apparatus (XY-105 MW, Changzhou Lucky Electronic Equipment, Changzhou, China). Concisely, 5 g of beef sausage were placed on a plate covered with aluminium foil and subjected to 100 °C. The water differences of the samples before and after mass were estimated using the equation below;

$$\text{Moisture loss (\%)} = \frac{W_0 - W_1}{W_0} \times 100 \quad (13)$$

Where  $W_0$  represents moisture content before weight and  $W_1$  represents moisture content after weight.

#### Microbiological determination

A modified method by Bassey et al. (2021) was adopted for gram-negative obligate aerobic bacteria *Pseudomonas* spp. and gram-positive facultative anaerobe non-spore-forming bacteria *Brochothrix thermosphacta* and the total viable count (TVC) of the packaged slice evaluation.

Briefly, 25 g samples were aseptically taken, minced, and transferred into sterile stomacher bags having 225 mL of 0.85% (m/v) sterile sodium chloride and homogenized for 120 s by employing a stomacher machine (BagMixer 8400 VW, Interscience Co., Bretesche, France). A serial dilution (1:10) was done and 0.1 mL diluent from each sample was inoculated on PCA to estimate the TVC via the pour plate method and incubated at 37 °C for 48 h. The CFC agar incorporated with culture medium supplement and incubated at 28 °C for 24 h was used to determine *Pseudomonas* spp. bacteria count. The STAA agar and incubated at 28 °C for 24 h was used to determine *B. thermosphacta* count. The colony-forming units (CFU/mL) results were changed logarithmically and then subjected to statistical analysis.

### Statistical analysis

The OriginLab software (version 12.5; OriginLab Corporation Northampton, Massachusetts, USA) was utilized to perform all analyses. A one-way analysis of variance (ANOVA) and Tukey's tests was applied in mean values of multiple comparisons among the experimental treatments to evaluate significant differences.

## Results and discussion

### Film antioxidant and antimicrobial activity

#### Film radical scavenging ability

An increase from 33.88% for CT to 69.44% for CG-KPE1, 85.84% for CG-KPE2, 93.55% for CG-KPE3 film and 12.43 for CT to 27.25% for CG-KPE1, 39.04% for CG-KPE2, 53.49% for CG-KPE3 film were observed for ABTS<sup>+</sup> (Fig. 1a) and DPPH (Fig. 1a) radical scavenging activities respectively. Further, the antioxidant capacity of CG-KPE films was enhanced by KPE inclusion due to polyphenols content in KPE. According to Haddad et al. (2020), the synergistic activity of phenolic groups (phenolic ring) influenced oxidation inhibition by delocalizing unpaired electrons and denoting hydrogen atoms from hydroxyl groups. Dias et al. (2020) reported the high antioxidant activity among the peels of kiwifruit varieties *Actinidia deliciosa* cv. "Hayward" (green) and *Actinidia* spp. (red). The antioxidative action of developed film was KPE dose-dependent, indicating an effective oxidation inhibition potential among CG-KPE films compared to CG-CT. Zamuz et al. (2021) reported that polyphenols enhanced the shelf-life of fresh minced beef, cooked ham, and pork burgers due to the compound's antioxidant capacity. Results corroborate with a similar study by Kaya et al. (2018) for utilizing *Pistacia terebinthus* stem, leaf, and seed extracts in chitosan-based antioxidative and antimicrobial films production for application

in food coating and packaging industry. Also, Alnadari et al. (2023a) reported similar results for incorporating anthocyanins from *Cinnamomum camphora* fruit peel in sodium carboxymethyl cellulose composite film for packaging beef and chicken slices.

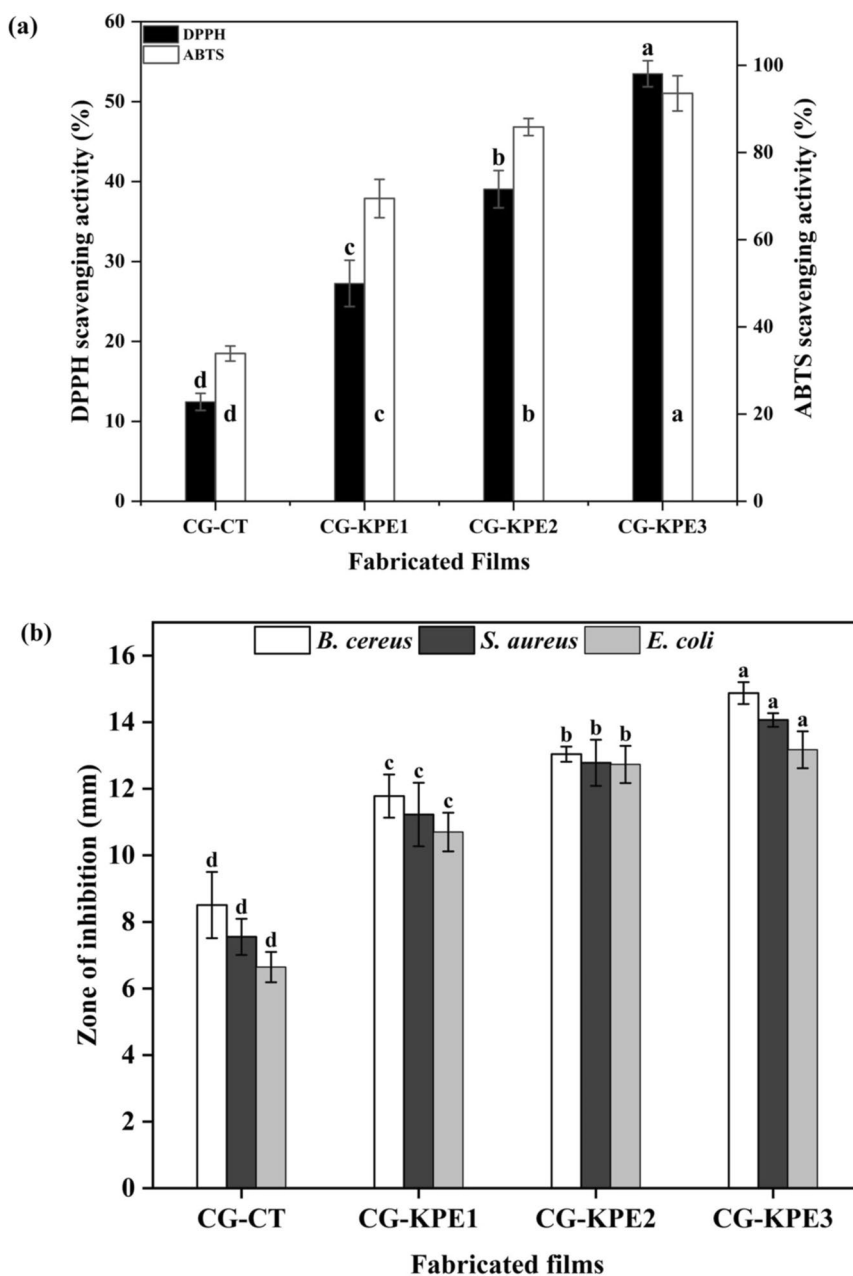
### Film antimicrobial activity

Figure 1(b) shows a significant microbial inhibitory action on tested food-borne pathogenic bacteria *Escherichia coli* (gram-negative) and *Staphylococcus aureus*, and *Bacillus cereus* (gram-positive) ( $p < 0.05$ ). The KPE concentrations impacted CG-KPE films disk inhibitory zones effectively compared to CG-CT. Thus, CMC interaction with KPE organic acid resulted in antimicrobial efficacy. Mastro-matteo et al. (2014) reported that organic acid penetrated and disrupted bacteria cell wall-normal physiology to impair or terminate bacteria growth due to a lower internal pH. Therefore, the *Escherichia coli*, *Staphylococcus aureus*, and *Bacillus cereus* showed a steady-less retarded growth within the CG-CT films. The numerous pores and easy cellular permeability of tested bacteria cell wall membrane rendered the superior antimicrobial activity of CG-KPE films. Dias et al. (2020) also reported the antimicrobial efficacy among kiwifruit peels. Hence, the KPE in CG-KPE films confirms the possible synergistic impact of antimicrobial action associated active film system due to the presence of phenolic compounds. Pateiro et al. (2019) reported the antimicrobial effectiveness of green tea extract and essential oregano oil in antioxidant active packaging system. In comparison to CG-CT, CG-KPE films revealed superior antimicrobial properties possibly to control food microbial actions similar to Chinese chive (*Allium tuberosum*) root extract based biodegradable active food packaging (Riaz et al., 2020).

### Film properties characterization

#### SEM

Figure 2 shows superficial film microstructures, voids, smoothness, homogeneity, layer structure, and cross-section matrix images. The SEM images showed microvoids and fractured areas in CG-CT composite film due to brittleness. GA might have influenced the CG-CT composite film structure and resulted in discontinuation in the polymer matrix. However, the KPE improved the smoothness, uniformity, and homogeneity of the CG-KPE composite film structures without bubbles or pores due to KPE polyphenolic compounds hydrophilicity characteristics and the traction force influenced by CG-KPE matrix after solvent evaporation, thus exhibiting a clear SEM micrograph. No vivid uniformly dispersed aggregation was noticed at low dosage (KPE 1%). In contrast, high KPE concentrations (2–3%) revealed better



**Fig. 1** (a) DPPH (2,2-Diphenyl-1-picrylhydrazyl) and ABTS<sup>+</sup> (2,2'-azino-bis-(3-ethylbenzothiazoline-6-sulphonic acid) scavenging activities of fabricated CG-CT (carboxymethyl cellulose and gum Arabic – control) and CG-KPE (carboxymethyl cellulose and gum Arabic –lyophilized kiwifruit peel powder extract) active films (b) CG-CT (carboxymethyl cellulose and gum Arabic – control) and CG-KPE (carboxymethyl cellulose and gum Arabic – lyophilized kiwifruit peel powder extract) active films inhibitory effects on three kinds of bacteria. Values are mean ± SD (n = 3), <sup>a-d</sup> represent significant differences (p < 0.05). CG-CT (carboxymethyl cellulose and gum Arabic – control film), CG-KPE1 (carboxymethyl cellulose and gum Arabic – 1% of lyophilized kiwifruit peel powder extract film), CG-KPE2 (carboxymethyl cellulose and gum Arabic – 2% of lyophilized kiwifruit peel powder extract film), and CG-KPE3 (carboxymethyl cellulose and gum Arabic – 3% of lyophilized kiwifruit peel powder extract film)

homogeneity with lighter spots which might be relative to improved film stability. Consequently, the SEM results extensively induced KPE-treated films tensile strength due to low transmittance values and enhanced softness compared to CG-CT. Also, the clear micrographs

of CG-KPE composite films could effectively impact the mechanical properties, water vapor, and oxygen inhibition by KPE even distribution in films. In similitude, Suriyatem et al. (2018) reported similar SEM results trend for

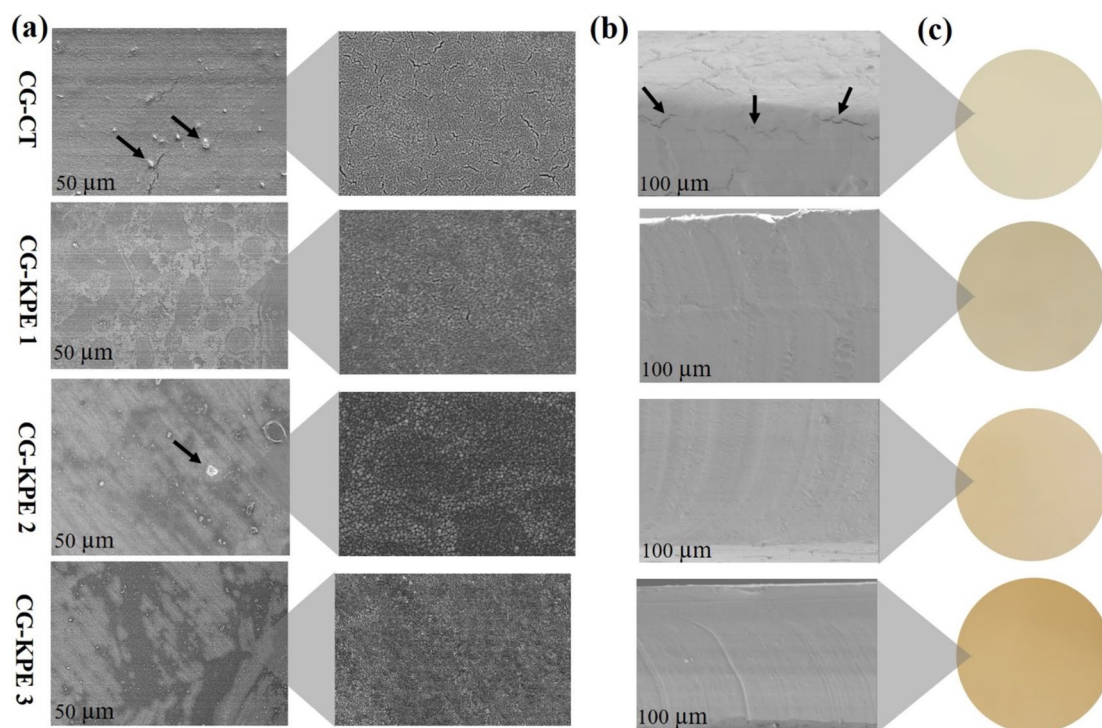


**Fig. 2** (a) Surface-sectioned SEM (Scanning electronic microscopy) (b) Cross-sectioned SEM (Scanning electronic microscopy) (c) Appearance of fabricated films. CG-CT (carboxymethyl cellulose and gum Arabic—control), CG-KPE1 (carboxymethyl cellulose and gum Arabic – 1% of lyophilized kiwifruit peel powder extract film), CG-KPE2 (carboxymethyl cellulose and gum Arabic – 2% of lyophilized kiwifruit peel powder extract film), and CG-KPE3 (carboxymethyl cellulose and gum Arabic – 3% of lyophilized kiwifruit peel powder extract film)

carboxymethyl chitosan blended with rice starch-based films.

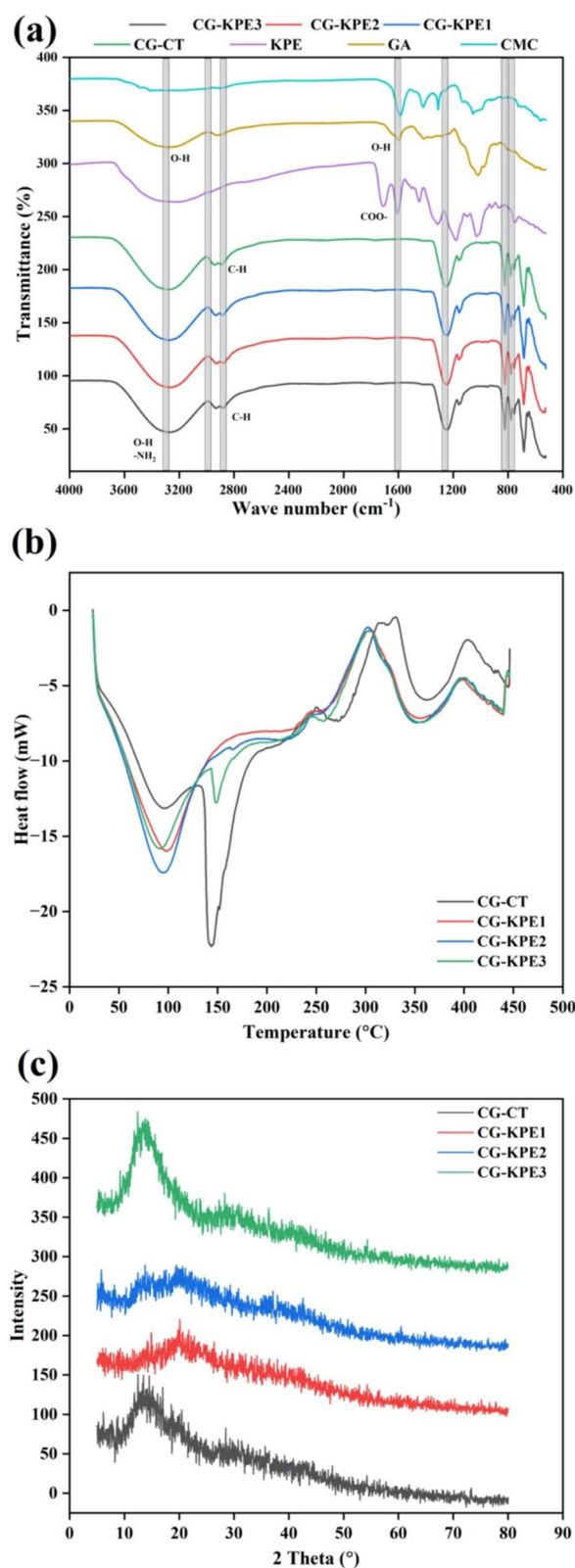
#### FTIR

Figure 3(a) shows the broad and strong spectral bands of films centered at  $3270\text{ cm}^{-1}$  (O–H stretching mode) intermolecular hydrogen bond and peaks at  $2926$  and  $2875\text{ cm}^{-1}$  corresponded to C–H extending from alkyl groups. Also, C=O bond stretching, N–H bending vibration, and C–N band extension conformed to  $1591$ ,  $1034$  and  $916\text{ cm}^{-1}$  peak discretely. The KPE-treated films showed a wavelength of about  $1601\text{ cm}^{-1}$  assigned to  $\text{COO}^-$  (symmetric) and  $1077\text{ cm}^{-1}$  relative to C–O–C stretching of principal points (Wu et al., 2013). On the other hand, CMC displayed  $3294\text{ cm}^{-1}$  (O–H),  $1589\text{ cm}^{-1}$  ( $\text{COO}^-$  (asymmetric),  $1418\text{ cm}^{-1}$  ( $\text{COO}^-$  (Symmetric), and  $1051\text{ cm}^{-1}$  (C–O–C) wavenumber length in principal points. Also, at  $2899\text{ cm}^{-1}$  threshold, aliphatic C–H stretching with an observed bending vibration band was detected similar to the study of Akhtar et al. (2018). Whereas, GA recorded a spectral band of  $1412\text{ cm}^{-1}$  (symmetrical) and  $600\text{ cm}^{-1}$  (asymmetric) correlating with  $\text{COO}^-$  stretching vibration (Xu et al., 2019). A  $3292\text{ cm}^{-1}$  spectral band denoted O–H extension, thus a characteristic of a glycosidic ring. Whereas  $2925\text{ cm}^{-1}$

signified C–H extension. Hence, in CG-CT film formation, CMC and GA mixture altered wavenumbers from  $3507$  to  $3004\text{ cm}^{-1}$  to yield a strong absorption for O–H stretching at  $3276.46\text{ cm}^{-1}$  band. Another peak was generated at  $2898\text{ cm}^{-1}$ , which was absent in the CMC or GA spectrum. This observation evidenced a cross-link reaction among CMC and GA during the composite film process. The low wavelength shift of some peaks of CG-KPE film could be related to KPE dose-dependent interactions in the glycerol-polymer matrix. Hence, the spectrum of CG-KPE films confirms successful interactions of KPE in the matrix.

#### DSC

All the film thermograms indicated two distinct peaks relative to exothermic and endothermic occurrences except CG-CT and CG-KPE3, which exhibited three peaks (Fig. 3b). Endothermic and exothermic properties of diverse thermal transitions were seen due to increased temperature. The residual moisture dehydration of CG-CT film by heat generated initial endothermic peaks ( $94.8$ ,  $147$  and  $364.6\text{ }^\circ\text{C}$ ), whereas the  $306.3\text{ }^\circ\text{C}$  exothermic peaks could be attributed to polysaccharide disintegration. Again, endothermic peaks centered at  $91.04$ ,  $152.4$  and  $356.16\text{ }^\circ\text{C}$  corresponded to CG-KPE films. In brief,



◀ **Fig. 3** (a) FTIR (Fourier transform infrared spectroscopy) spectra of film composite ingredient CMC (carboxymethyl cellulose), GA (gum Arabic), KPE (lyophilized kiwifruit peel powder extract), CG-CT (carboxymethyl cellulose and gum Arabic – control) film, and CG-KPE (carboxymethyl cellulose and gum Arabic – lyophilized kiwifruit peel powder extract) composite films (b) Films DSC (Differential scanning calorimetry) thermograms (c) Films X-RD (X-ray diffraction) pattern. CG-CT (carboxymethyl cellulose and gum Arabic – 1% of lyophilized kiwifruit peel powder extract film), CG-KPE1 (carboxymethyl cellulose and gum Arabic – 2% of lyophilized kiwifruit peel powder extract film), and CG-KPE3 (carboxymethyl cellulose and gum Arabic – 3% of lyophilized kiwifruit peel powder extract film)

KPE modified the structure formation between CMC and GA polymers to induce the strong thermal stability of CG-KPE films compared to CG-CT. This is because the number of hydroxyls in CMC and GA could be reduced by KPE for strong hydrogen bonds to be established between polymers. Volf et al. (2014) reported thermal stability among standard polyphenols (catechin, gallic acid, and vanillic acid) and natural polyphenols from spruce bark and grape seeds. Hence, KPE polyphenols could be relative to the increased thermal stability properties of CG-KPE films. Also, the high thermal stability among KPE developed films reveals similar effect of the bio-composite film properties of sodium CMC-GA/anthocyanins from *Cinnamomum camphora* fruit peel biopolymer-based dehydration film developed for beef and chicken meat preservation (Alnadari et al., 2023a).

#### XRD

A shapeless crystalline structure with a wider and one peak presence at  $2\theta$  about  $14^{\circ}$  was observed among CG-CT diffractogram in Fig. 3(c). This was in tandem with the cellulose-starch-ZnCl<sub>2</sub> hybrid films by the report of Shang et al. (2019). CG-CT film inner structure detected no defect. KPE inclusion only displayed a reduction in the strength of spectral peaks. The X-ray spectrum of CG-KPE films became broader with increased KPE concentration. Consequently, CMC, GA, and KPE interaction aided the phenomenon of hydrogen bonds in composite films, thus a decline in crystallinity. Film mechanical attributes rely dynamically on the crystallites in its structure. Also, the competitive effect of the hydrogen bonds between CG-CT and KPE interactions to an extent hindered the formation of CG-CT inter- and intra-molecular hydrogen bonds, resulting in low crystallinity of CG-CT film. It is noteworthy that hydrogen bonds among composite materials improved the peaks intensity of the developed films. Suriyatem et al. (2018) reported similar findings of good compatibility of rice-starch component blended film coupled with a good miscibility of

intermolecular interaction of developed film evidenced by FTIR. Hence, crystal structure degree of CG-KPE films exerted an enhanced trend. Currently, there are no available reports detailing XRD analysis of KPE composition in composite film. Therefore, the finding provides valuable insights into the crystallinity characteristics to aid the understanding of KPE properties and potential for active packaging applications.

### Film physical and mechanical characteristics

#### Film swelling degree, water solubility, and moisture content

A significant decline ( $p < 0.05$ ) in swelling, water content, and water solubility values were observed in CG-KPE films, as shown in Table 1. According to Wu et al. (2013), water diffusion, polymer relation, ionic and hydrogen bond dissociation, and amino group ionization were linked to film swelling. CG-CT exhibited a high-water solubility (easy water interaction), whereas KPE incorporation improved water-resistant characteristics in CG-KPE composite films. Possible reason could be associated to the mechanism of molecule hydrophilic (carboxylic groups) intrinsic swelling phenomenon CG-CT films as reported by Hafsa et al. (2016). Also, CG-KPE films were KPE dose-dependent due to a decreased water-solubility properties conjugated to hydrogen bond interaction between CG-KPE

matrixes. Consequently, fabricated film integrity and water resistance determinants revealed a significantly decreased (26.77 to 18.62%) water content in CG-KPE compared to CG-CT probably due to electrostatic interactions (Xu et al. 2019). Wang et al. (2019a, 2019b) noticed similar results supporting this study among *Herba Lophatheri* extract fabricated active films.

#### Color and opacity

Table 2 reveals that color and opacity were influenced among CG-KPE composite films due to KPE compared to CG-CT. Thus, the color and the opacity of food packaging material play an integral role in directly influencing food appearance and consumer purchase decisions. Color indicators ( $L^*$ ,  $a^*$ , and  $b^*$ ) recorded a significant variation ( $p < 0.05$ ) as CG-CT films (brownish-white) were extremely transparent. At the same time, KPE green pigmentation to an extent, resulted in the opaque state of KPE-treated films (brownish-green). Likewise,  $\Delta E$  and YI increased, whereas WI decreased. An observable KPE dose-dependent was seen as CG-KPE3 transmitted an extra light brownish-green compared to CG-KPE1 and CG-KPE2. Thus, high opacity and less transparency in the CG-KPE films network polymer alignment were relative to transmittance. Hence, CG-KPE films could be suitable to keep meat color stable and control photo-oxidative

**Table 1** Physical properties of films

Film sample	Thickness (mm)	Swelling degree (%)	Solubility (%)	Moisture content (%)
CG-CT	0.07 ± 0.02 <sup>a</sup>	84.12 ± 4.18 <sup>a</sup>	46.15 ± 0.46 <sup>a</sup>	26.77 ± 0.46 <sup>a</sup>
CG-KPE1	0.07 ± 0.02 <sup>a</sup>	77.73 ± 1.01 <sup>b</sup>	42.11 ± 1.20 <sup>b</sup>	21.15 ± 2.49 <sup>b</sup>
CG-KPE2	0.07 ± 0.00 <sup>a</sup>	72.34 ± 0.52 <sup>c</sup>	39.91 ± 0.18 <sup>b</sup>	19.18 ± 1.99 <sup>b</sup>
CG-KPE3	0.08 ± 0.02 <sup>a</sup>	66.58 ± 0.27 <sup>d</sup>	36.57 ± 1.46 <sup>c</sup>	18.62 ± 2.60 <sup>b</sup>

Values are mean ± SD (n=3)

Different letters (a-d) in the same column indicate significant differences ( $p < 0.05$ )

CG-CT (carboxymethyl cellulose and gum Arabic – control film), CG-KPE1 (carboxymethyl cellulose and gum Arabic – 1% of lyophilized kiwifruit peel powder extract film), CG-KPE2 (carboxymethyl cellulose and gum Arabic – 2% of lyophilized kiwifruit peel powder extract film), and CG-KPE3 (carboxymethyl cellulose and gum Arabic – 3% of lyophilized kiwifruit peel powder extract film).

**Table 2** Color and opacity of films

Film sample	$L^*$	$a^*$	$b^*$	$\Delta E$	YI	WI	Opacity (mm <sup>-1</sup> )
CG-CT	83.23 ± 0.47 <sup>a</sup>	-0.47 ± 0.17 <sup>d</sup>	1.30 ± 0.91 <sup>c</sup>	11.86 ± 0.37 <sup>c</sup>	2.23 ± 1.56 <sup>d</sup>	83.16 ± 0.53 <sup>a</sup>	1.81 ± 0.22 <sup>d</sup>
CG-KPE1	68.09 ± 0.62 <sup>b</sup>	1.77 ± 1.00 <sup>c</sup>	12.05 ± 1.54 <sup>b</sup>	29.67 ± 2.65 <sup>b</sup>	25.27 ± 3.45 <sup>c</sup>	65.83 ± 1.15 <sup>b</sup>	7.65 ± 0.57 <sup>c</sup>
CG-KPE2	66.64 ± 0.64 <sup>b</sup>	3.16 ± 0.46 <sup>b</sup>	16.68 ± 2.74 <sup>a</sup>	32.73 ± 1.89 <sup>b</sup>	35.77 ± 5.71 <sup>b</sup>	62.51 ± 1.15 <sup>c</sup>	9.32 ± 0.80 <sup>b</sup>
CG-KPE3	60.24 ± 1.74 <sup>c</sup>	5.26 ± 0.58 <sup>a</sup>	19.34 ± 0.25 <sup>a</sup>	39.32 ± 1.66 <sup>a</sup>	45.87 ± 1.54 <sup>a</sup>	55.47 ± 1.65 <sup>d</sup>	12.52 ± 0.36 <sup>a</sup>

Values are mean ± SD (n=3)

Different letters (a-d) in the same column indicate significant differences ( $p < 0.05$ )

CG-CT (carboxymethyl cellulose and gum Arabic – control film), CG-KPE1 (carboxymethyl cellulose and gum Arabic – 1% of lyophilized kiwifruit peel powder extract film), CG-KPE2 (carboxymethyl cellulose and gum Arabic – 2% of lyophilized kiwifruit peel powder extract film), and CG-KPE3 (carboxymethyl cellulose and gum Arabic – 3% of lyophilized kiwifruit peel powder extract film)

deterioration relative to the dosage employed. The present color and opacity findings corroborate with several studies among the wide application of carboxymethyl and GA in the fabrication of packaging materials based on Chinese chive (*Allium tuberosum*) (Riaz et al., 2020), *Cinnamomum camphora* seed extract (Alnadari et al., 2022), anthocyanin from *Cinnamomum camphora* fruit peel (Alnadari et al., 2023a; Alnadari et al. (2023b)).

#### **Thickness**

Generally, no significant difference in film thickness was noticed in values ranging between 0.08 and 0.07 mm (Table 1). Cheng et al. (2015) reported a similar result of film thickness amidst the distribution of phenolic in film internal domains. Instead, an improved film tensile strength and soft elasticity were detected. Thus, KPE polyphenol interaction with CG-GA could have resulted in strong molecular bonds between polyphenols and GA. Also, the continuous stirring in tandem with pulverized content addition, film matrix organized structure interruption and increased KPE concentration could have generated molecules close to each other (nanoscale-quasi). Hydrogen bonds are known to be easily generated among similar polysaccharide structures (Kang et al., 2021b). Hence, polysaccharides' hydrogen bond and hydrophobic force interactions within CG-KPE caused the tighter binding matrix, which induced film structure and surface smoothness.

#### **Mechanical properties**

An increased TS and EB values of films are shown in Fig. 4(b). TS values centered between 41.61% and 34.14 MPa, while 59.17% and 40.49 MPa range corresponded to EB and TS respectively. These results could be attributed to the interaction of KPE polyphenolic polar characteristics with CG hydrophilic groups which resulted in a cross-linking in CG-KPE mechanical strength and extensibility modification. While, CG-CT film exhibited a low mechanical strength property. Qin et al. (2019) reported results in conformity to the present study with the intermolecular hydrogen bond formation of OH groups in CMC and GA causing a stronger interfacial adhesion between CG-KPE films. Also, feeble attractive forces facilitate polymeric chain movement leading to the elongation break (fracture strain) (Qin et al., 2019). According to Wang et al. (2019a, 2019b), film's mechanical property is dependent on crystallite presence, polymer composition, electrostatic, and intermolecular interaction. The homogeneity of CG-KPE films conform with KPE dose influence in the mechanical properties. Therefore, KPE influenced CG-KPE compact inner structure to maintain film physical integrity for potential application as a meat package.

#### **Films bioactivities**

##### **Biodegradation**

Figure 4(a) showed a significant weight loss among CG-KPE composite films compared to CG-CT in correspondence to bioactivity progression ( $p < 0.05$ ). After 3 weeks, CG-KPE recorded the maximum degradation loss of about 57.70%, whereas CG-CT films noticed the lowest bioactivity values ranged between 45.0%-47.7%. This could be interpreted as KPE incorporation in CG generated a hybrid polymeric material which was quick to be degraded. Also, heat, moisture, and enzyme action in the soil influenced film integrity for disintegration. Similar bio-disintegration result likened to this study include rosemary extract-cassava starch composite film (Piñeros-Hernandez et al., 2017) and chitosan-based Chinese chive root extract biodegradable film (Riaz et al., 2020). The marked findings of the biological degradation estimation showed that KPE incorporation enhanced CG-KPE film bioactivities.

#### **Films application for beef sausage slices**

##### **Color**

Accordingly, the  $L^*$  values declined among sample groups with increased storage period (Fig. 5). The minimum value of  $L^*$  was recorded among the T3 treatment. Also, samples revealed the reduced value of  $a^*$  during storage possibly due to the KPE absence in CT in relation to less opacity. Significant differences were seen across the storage days, among d 6, 9 and 12 treatments. A decreased trend of  $b^*$  color index was realized among samples at d 12 compared to d 0, 3, 6 and 9.

Generally, the synergic effect of KPE doses in developed films significantly impacted packaged sausage-slice color with storage time. Thus, significant differences were evidenced on d 6, 9 and 12 for  $L^*$  and  $a^*$  indexes and d 12  $b^*$  index. According to Deus et al. (2017), the absorbance ability and the specific light wavelength scattering were influenced by particle color to generate differences among pigments. However, the CG-KPE film composition interacted positively with the beef sausage slices due to KPE polyphenolics ability in stabilizing product color during storage. In brief, an increased KPE dose altered the opacity of the films thereby decreasing the effect of packaged products photo oxidation caused by the film transparency as revealed and complement TBARS results among packaged sausages. Thus, sausages color change, nutritional loss, and off-flavor during shelf-life period could be controlled.

##### **pH and moisture content**

A rise in pH contributes to the formation of byproducts like ammonia, dimethylamine, and trimethylamine by spoilage meat microorganism (Alnadari et al.,

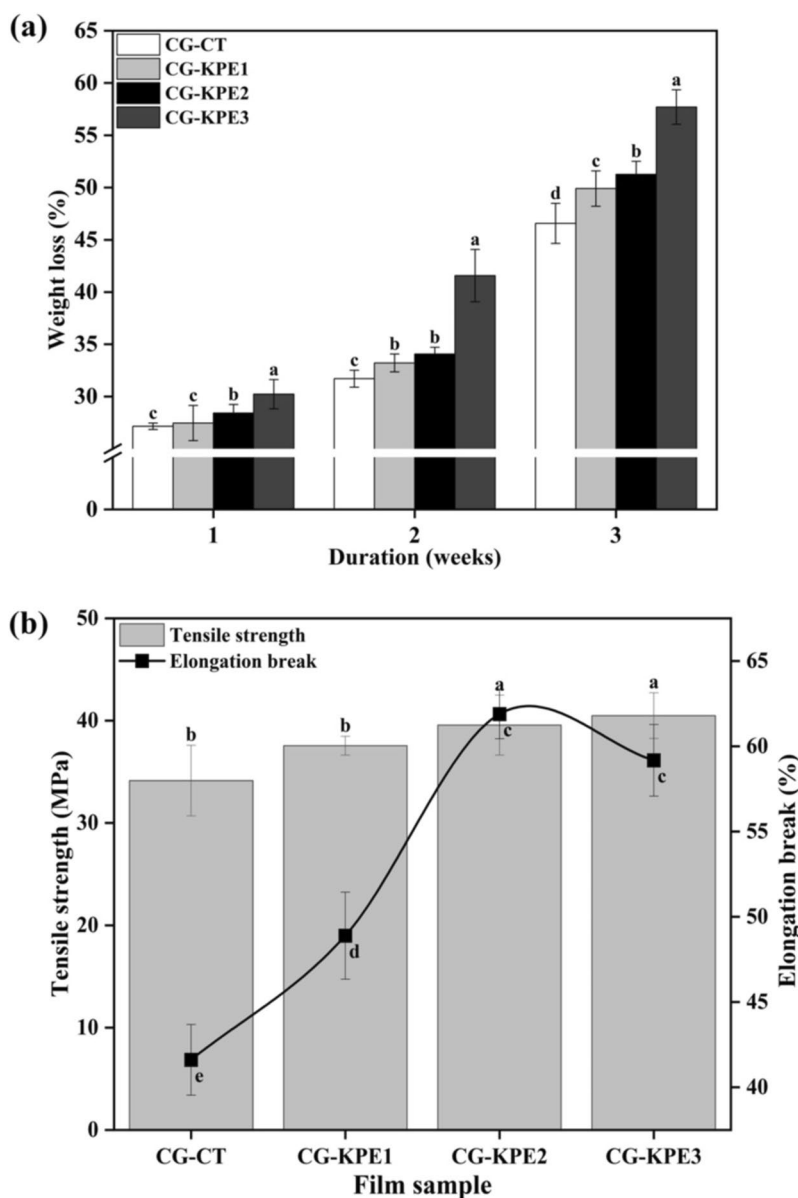


**Fig. 4** (a) Films biodegradability evaluation (b) Films mechanical properties

2023b). Therefore, pH values in Fig. 6(a) indicated significantly different results among treatments and was directly proportional to increased storage time. Slightly high pH values were recorded at d 0 while d 12 recorded the least pH values among T1, T2, and T3 samples compared to CT samples. These changes could be interpreted as KPE polyphenolic acid efficacy within CG-KPE films effectively regulated T1, T2, and T3 samples pH during storage. Also, KPE presence in the developed films interacted with the sample's environment, which was relatively constant to control pH effectively during storage. The result corroborates with

Pateiro et al. (2019) report that the diminution of pH had a relation to the microbial growth and the dissolution of CO<sub>2</sub> from the packaged system. In brief, the KPE generated an acidic condition that influenced the antimicrobial efficacy of the film on the packaged product to positively reduce the pH effect on package products during storage.

Moisture content is a major intrinsic factor that influences microbial deterioration and consequent economic losses of processed meat products (Zhang et al., 2010). However, product water loss control is a primary function of packaging materials for shelf-life, quality

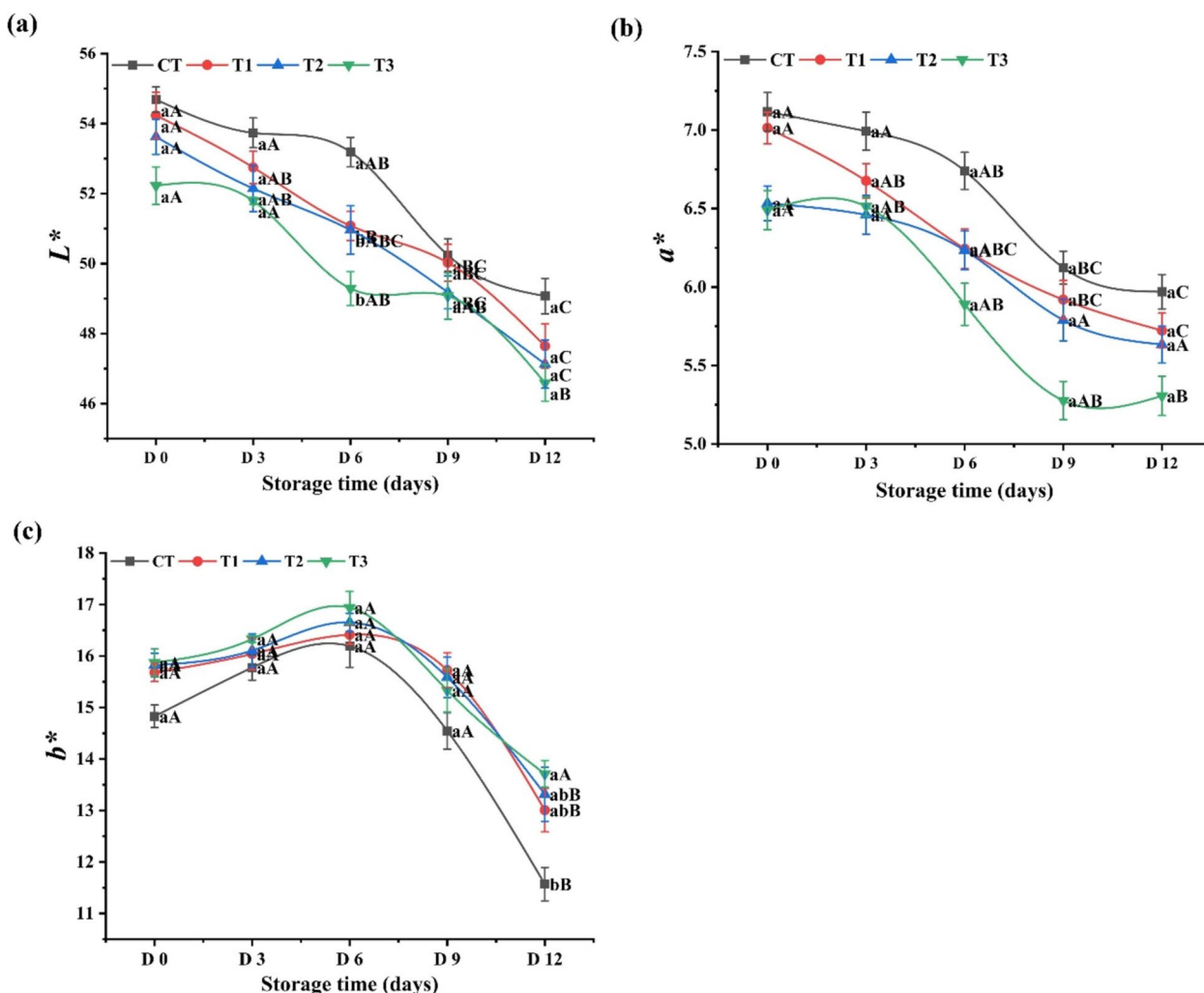


**Fig. 5** (a) Lightness (b) Redness (c) Yellowness results of packaged beef sausage slices during 12 d of refrigerated storage. Values are mean  $\pm$  SE ( $n=3$ ). <sup>a–e</sup> Means values are significantly different ( $p < 0.05$ ) across the treatments. Whiles <sup>A–D</sup> means values are significantly different ( $p < 0.05$ ) across the storage duration. CT: Control (CG-CT (carboxymethyl cellulose and gum Arabic – control film)), T1 (Treatment 1): (CG-KPE1 (carboxymethyl cellulose and gum Arabic – 1% of lyophilized kiwifruit peel powder extract film)), T2 (Treatment 2): (CG-KPE2 (carboxymethyl cellulose and gum Arabic – 2% of lyophilized kiwifruit peel powder extract film)), and T3 (Treatment 3): (CG-KPE3 (carboxymethyl cellulose and gum Arabic – 3% of lyophilized kiwifruit peel powder extract film))

purposes, and foggy film formation prevention (Ozdemir & Floros, 2004). Hence, in Fig. 6(b), a steady decline in water content was seen among the treated samples during storage without significant variation noticed among treatments. The results could be attributed to the hydrophilic nature of plant origin CG-KPE film composition (Zhao et al., 2019). Interestingly, the moisture content values revealed no variations among experimental treatments. This evidences the functional ability of CG-KPE films synergetic impact on packaged samples physico-chemical quality. Concisely, the results suggested that KPE within CG-KPE composite films could control the

pH and moisture content of package beef sausage slices to maintain the chemical stability of the products.

**Texture**

Table 3 shows the effect of developed CG-KPE films for packaging beef slices during 12 d refrigerated storage. Meat product texture influences consumers’ acceptability (Gao et al., 2014). Comparatively, no significant difference was observed in hardness values among treatments, yet hardness increased progressively by storage period. Therefore, the higher hardness values could be linked to the shortening of protein distance due to the possible loss of water content influencing the

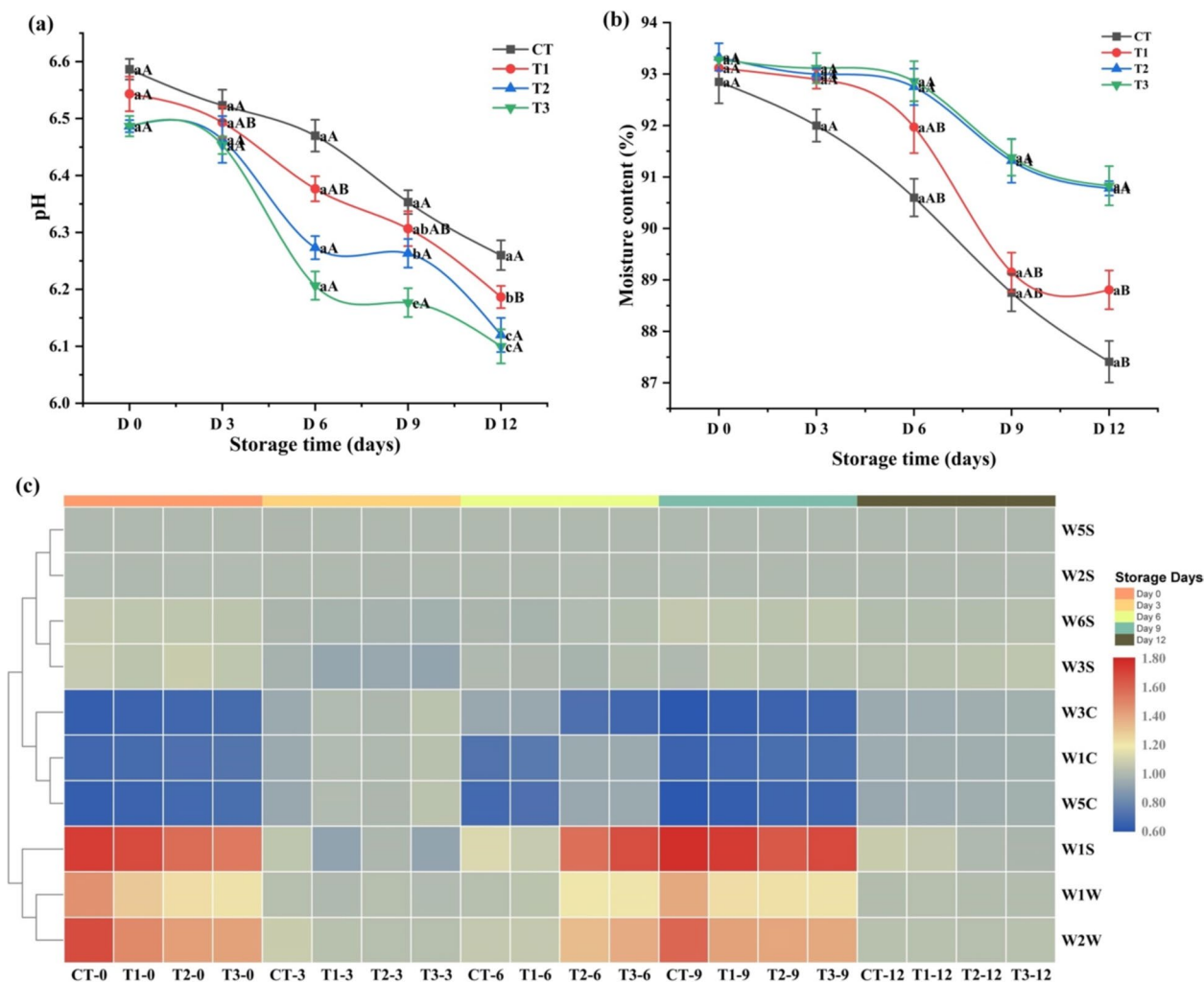


**Fig. 6** (a) pH (b) moisture content (c) E-nose cluster heat map results of packaged beef sausage slices during 12 d of refrigerated storage. Values are mean  $\pm$  SE ( $n=3$ ). <sup>a-e</sup> Means values are significantly different ( $p < 0.05$ ) across the treatments. While <sup>A-D</sup> means values are significantly different ( $p < 0.05$ ) across the storage duration. CT: Control (CG-CT (carboxymethyl cellulose and gum Arabic – control film)), T1 (Treatment 1): (CG-KPE1 (carboxymethyl cellulose and gum Arabic – 1% of lyophilized kiwifruit peel powder extract film)), T2 (Treatment 2): (CG-KPE2 (carboxymethyl cellulose and gum Arabic – 2% of lyophilized kiwifruit peel powder extract film)), and T3 (Treatment 3): (CG-KPE3 (carboxymethyl cellulose and gum Arabic – 3% of lyophilized kiwifruit peel powder extract film))

formation of new cross bond of protein (Arjenaki et al., 2019). Thus, the results confirm CG-KPE films ability to check water retention of packaged products. There were no significant differences among all treatments for chewiness revealing a greater force demand to chew products. Resilience values obtained for T3, T1, and T2 samples were slightly high compared to CT. Also, springiness and cohesiveness noticed no significant difference among treatments. According to Wang, Qiu, & Zhu (2021), KPE is a plant source for phenolic additive that possesses an exogenous texturizing agent or proteolytic cysteine actinidin ability to tenderize meat. However, KPE incorporation in CMC-GA improved the

functionality of the film to influence the matrices of T1, T2, and T3 packaged products during storage. Thereby, these results indicate a non-adverse impact of CG-KPE films use on product textural properties.

**Electronic nose**

The E-nose classification pattern generally revealed a significant sensor response (Table 4) among all treatments and flavor relative to the storage days. Also, Fig. 6(c) sensor response pattern in cluster heat-map revealed a fluctuating response of volatile organic compounds (VOCs) treatments during storage. Treatment’s sensory array responses at d 3 and 12 were similarly lower than d 0 and

**Table 3** Textural properties of packaged sliced-beef sausages

Storage time (days)	Treatments			
	CT	T1	T2	T3
<b>Hardness (g)</b>				
D 0	10547.97 ± 912.05 <sup>aA</sup>	10087.64 ± 840.46 <sup>aB</sup>	9790.68 ± 2364.11 <sup>aA</sup>	11121.10 ± 1956.37 <sup>aB</sup>
D 3	11460.77 ± 1696.29 <sup>aA</sup>	10729.68 ± 1683.25 <sup>aB</sup>	10389.64 ± 1983.78 <sup>aA</sup>	13017.11 ± 3512.14 <sup>aB</sup>
D 6	14589.82 ± 7145.08 <sup>aA</sup>	15565.67 ± 5732.13 <sup>aAB</sup>	14311.43 ± 1891.14 <sup>aA</sup>	13247.05 ± 2166.20 <sup>aB</sup>
D 9	15698.82 ± 857.39 <sup>aA</sup>	16788.05 ± 776.02 <sup>aAB</sup>	16619.51 ± 7725.64 <sup>aA</sup>	25928.14 ± 2934.22 <sup>aA</sup>
D 12	15511.36 ± 5513.59 <sup>aA</sup>	19693.40 ± 1585.20 <sup>aA</sup>	19584.74 ± 1573.13 <sup>aA</sup>	21147.94 ± 1213.52 <sup>aA</sup>
<b>Springiness</b>				
D 0	0.86 ± 0.02 <sup>aA</sup>	0.86 ± 0.05 <sup>aA</sup>	0.88 ± 0.05 <sup>aA</sup>	0.92 ± 0.02 <sup>aA</sup>
D 3	0.82 ± 0.06 <sup>aA</sup>	0.92 ± 0.01 <sup>aA</sup>	0.92 ± 0.03 <sup>aA</sup>	0.92 ± 0.05 <sup>aA</sup>
D 6	0.82 ± 0.04 <sup>aA</sup>	0.90 ± 0.02 <sup>abA</sup>	0.95 ± 0.07 <sup>aA</sup>	0.93 ± 0.03 <sup>abA</sup>
D 9	0.85 ± 0.05 <sup>aA</sup>	0.90 ± 0.03 <sup>aA</sup>	0.92 ± 0.03 <sup>aA</sup>	0.93 ± 0.04 <sup>aA</sup>
D 12	0.88 ± 0.03 <sup>aA</sup>	0.87 ± 0.02 <sup>aA</sup>	0.91 ± 0.03 <sup>aA</sup>	0.91 ± 0.03 <sup>aA</sup>
<b>Cohesiveness</b>				
D 0	0.70 ± 0.01 <sup>aA</sup>	0.71 ± 0.01 <sup>aA</sup>	0.70 ± 0.02 <sup>aA</sup>	0.71 ± 0.01 <sup>aA</sup>
D 3	0.71 ± 0.08 <sup>aA</sup>	0.71 ± 0.01 <sup>aA</sup>	0.72 ± 0.03 <sup>aA</sup>	0.72 ± 0.03 <sup>aA</sup>
D 6	0.68 ± 0.02 <sup>aA</sup>	0.70 ± 0.07 <sup>aA</sup>	0.72 ± 0.01 <sup>aA</sup>	0.73 ± 0.02 <sup>aA</sup>
D 9	0.72 ± 0.01 <sup>aA</sup>	0.71 ± 0.02 <sup>aA</sup>	0.73 ± 0.01 <sup>aA</sup>	0.75 ± 0.01 <sup>aA</sup>
D 12	0.71 ± 0.01 <sup>aA</sup>	0.70 ± 0.01 <sup>aA</sup>	0.72 ± 0.02 <sup>aA</sup>	0.72 ± 0.02 <sup>aA</sup>
<b>Chewiness (g)</b>				
D 0	6908.28 ± 1254.25 <sup>aA</sup>	6150.75 ± 858.61 <sup>aB</sup>	5992.37 ± 1280.30 <sup>aA</sup>	6840.41 ± 1340.29 <sup>aB</sup>
D 3	9085.37 ± 1136.88 <sup>aA</sup>	6964.73 ± 902.68 <sup>aB</sup>	7647.10 ± 1566.08 <sup>aA</sup>	8455.47 ± 1597.87 <sup>aB</sup>
D 6	5822.37 ± 560.24 <sup>aA</sup>	8763.59 ± 1140.69 <sup>aB</sup>	9658.33 ± 3710.57 <sup>aAB</sup>	10047.65 ± 1941.59 <sup>aA</sup>
D 9	9684.36 ± 4427.80 <sup>aA</sup>	10704.12 ± 478.11 <sup>aAB</sup>	11043.05 ± 4728.47 <sup>aA</sup>	15426.76 ± 1161.33 <sup>aA</sup>
D 12	10197.98 ± 3992.73 <sup>aA</sup>	12061.54 ± 997.66 <sup>aA</sup>	12939.92 ± 604.86 <sup>aA</sup>	12991.72 ± 418.70 <sup>aA</sup>
<b>Resilience</b>				
D 0	0.27 ± 0.01 <sup>bA</sup>	0.28 ± 0.01 <sup>bA</sup>	0.27 ± 0.01 <sup>bA</sup>	0.31 ± 0.01 <sup>aA</sup>
D 3	0.27 ± 0.05 <sup>aA</sup>	0.27 ± 0.02 <sup>aA</sup>	0.29 ± 0.02 <sup>aA</sup>	0.28 ± 0.02 <sup>aAB</sup>
D 6	0.25 ± 0.01 <sup>bA</sup>	0.28 ± 0.01 <sup>aA</sup>	0.29 ± 0.01 <sup>aA</sup>	0.28 ± 0.01 <sup>aAB</sup>
D 9	0.30 ± 0.03 <sup>aA</sup>	0.28 ± 0.01 <sup>aA</sup>	0.30 ± 0.02 <sup>aA</sup>	0.29 ± 0.01 <sup>aAB</sup>
D 12	0.30 ± 0.01 <sup>aA</sup>	0.30 ± 0.02 <sup>aA</sup>	0.28 ± 0.01 <sup>aA</sup>	0.28 ± 0.01 <sup>aB</sup>

Values are mean ± SD (n=3)

<sup>a,b</sup> Means values are significantly different ( $p < 0.05$ ) across the treatments. While <sup>A-B</sup> means values are significantly different ( $p < 0.05$ ) across the storage duration.

CT Control (CG-CT (carboxymethyl cellulose and gum Arabic – control film)), T1 (Treatment 1): (CG-KPE1 (carboxymethyl cellulose and gum Arabic – 1% of lyophilized kiwifruit peel powder extract film)), T2 (Treatment 2): (CG-KPE2 (carboxymethyl cellulose and gum Arabic – 2% of lyophilized kiwifruit peel powder extract film)), and T3 (Treatment 3): (CG-KPE3 (carboxymethyl cellulose and gum Arabic – 3% of lyophilized kiwifruit peel powder extract film)).

6. Day 9 recorded high VOC responses. Sensory array trend of CT treatments was profound towards the chemical sensors sensitive to W2W, W1W, and W1S at d 0, 3 and 9 compared to KPE film treatments.

Conversely, CG-KPE film treatment revealed an aroma response pattern towards the chemical sensors W5C and W6S throughout the storage days compared to CT samples. A unique pattern of VOCs towards chemical sensors W1C was high at d 3 while other days could not show a repetition of such pattern. Katiyo et al. (2020) reported that meat spoilage is related to sensory alterations. Hence, the d 3 fluctuated aroma profile corresponds with

d 3 microbial results reported in the study. The onset of microbial proliferation activities at d 3 influenced the fluctuating e-nose pattern by interfering with aroma sensitivity responses. Again, a relatively low sensor response target was noticed among W3S, W5S, and W2S. CT treatments sensors W3C were low at d 0 but increased with storage days with being predominant at d 3. The aroma of additives (spices) added in the formulated beef sausages also contributed to the high aroma profile of CT treatments during d 0, 3 and 9 storages. Some VOCs are meat spoilage indicators. However, other factors such as bacteria species and storage temperature could have

**Table 4** Information on ten chemical sensor array response

Chemical sensor	Chemical sensor class	Descriptions
W1S	Broad methane	Sensitive to methane
W5S	Broad range	Sensitive to nitrogen oxide
W1W	Sulfur-organics	Sensitive to organic-sulfides
W6S	Hydrogen	Sensitive to hydrogen compounds
W3S	Methane-aliph	Sensitive to methane and aliphatic
W3C	Aromatic	Sensitive to ammonia, aromatic molecules
W2S	Broad alcohols	Sensitive to alcohols, ketones, and aldehydes
W1C	Aromatic	Sensitive to aromatic and benzene compounds
W2W	Sulfur-chlor	Sensitive to organic-sulfides and organic-chloride
W5C	Aromatic-aliph	Sensitive to methane, propane, and aliphatic non-polar molecules

led to the inconsistent exposure of treatments to some chemical sensors at d 3 and 6. KPE presence in the CG-KPE film matrices successfully yielded chemical reactions VOCs in a packaged slices environment. Thus, these results suggest a higher aroma sensitivity trend of CG-KPE film treatments compared to CG-CT treatments. T3 recognized a slightly high VOCs sensor pattern than T1 and T2, comparatively, showing a KPE dose-dependent relative to higher VOCs. The results revealed the impact of CG-KPE films to exert VOCs to enhance intrinsic sensory attributes among packaged sliced-sausages. Zamuz et al. (2021) reported that polyphenol-rich extract influence sensory characteristics of raw and cooked meatballs and beef burger products.

#### Antimicrobial

A steady rise from the initial storage days in values ranging from 3.30 to 6.0 log CFU/g (TVC), 2.7 to 5.1 log CFU/g (*Pseudomonas* spp.), and 2.4 to 4.9 log CFU/g (*B. thermosphacta*) among treatments at the end of storage were revealed (Fig. 7). A steadily rising trend in TVC and *Pseudomonas* spp. count was noticed. In contrast, the trend of *B. thermosphacta* differed such that, CT and the KPE film treatments exhibited a lower counts of *B. thermosphacta* during storage. The *B. thermosphacta* count reached the highest level (4.9 log CFU/g), and was significantly lower than the *Pseudomonas* spp. (5.1 log CFU/g). On the other hand, TVC results trend indicate that the packaged samples were relative to KPE dose incorporated in film. This result could be associated with the cell wall structure, shape, and spore-forming ability of *B. thermosphacta* and *Pseudomonas* spp., making KPE activity more effective in developed films more effective. A similar result was reported among clove oil fabricated films action against *S. aureus* and *B. aureus* of ground chicken meat (Muppalla et al., 2014). Yang et al. (2019) reported a narrow antibacterial spectrum ability of Plastaricin BM-1

coated active plastic multilayer films against *Listeria monocytogenes* in a trypticase soy-yeast extract broth culture among chilled meat. However, CMC-ZnO based film effectively exhibited intrinsic antimicrobial ability and tested foodborne pathogenic bacteria *E. coli* and *L. monocytogenes* activity was inhibited by the presence of ZnO by disrupting *E. coli* completely after 9 h of culturing (Roy & Rhim, 2020). According to Ye et al. (2008), the antimicrobial action of fabricated chitosan-coated plastic films depended on the ham steak product matrix. Therefore, the antimicrobial efficacy was less effective in the CT film's treatments. Thus, CMC interaction with KPE organic acid results in antimicrobial efficacy. Mastromatteo et al. (2014) reported that organic acid penetrated and disrupted bacteria cell wall-normal physiology to terminate bacteria growth due to a lower internal pH. Therefore, the TVC, *B. thermosphacta*, and *Pseudomonas* spp. showed a steady-less retarded growth within the CT treatments during storage. The present result corroborates with *Pseudomonas* spp. inhibition during 10 d of storage at 4 °C (Yang et al., 2019) and the reduced count of *Pseudomonas* spp. among beef samples treated with free oil essential films (Arvanitoyannis & Stratakis, 2012). Concerning the TVC, a delay in the microbial rise was seen among CT and T1 treatments at d 6 compared to T2 and T3 samples. This could be related to the pH effect and dissolution of CO<sub>2</sub> in packaged film environment among CT and T1 samples. Moreover, KPE bioactive compounds possibly interacted with the packaged matrices by exerting antimicrobial agents into the sliced-beef sausages during storage via a migration mechanism. Phenolic compounds such as rutin, caffeic acid, hydroxybenzoic acid, quercetin, protocatechuic acid were reported to be found in kiwifruit peel (Boateng et al., 2022). The KPE inhibited TVC, declined *B. thermosphacta* count at d 9, and rendered *Pseudomonas* spp. stationary after d 9. Conclusively, Siripatrawan and

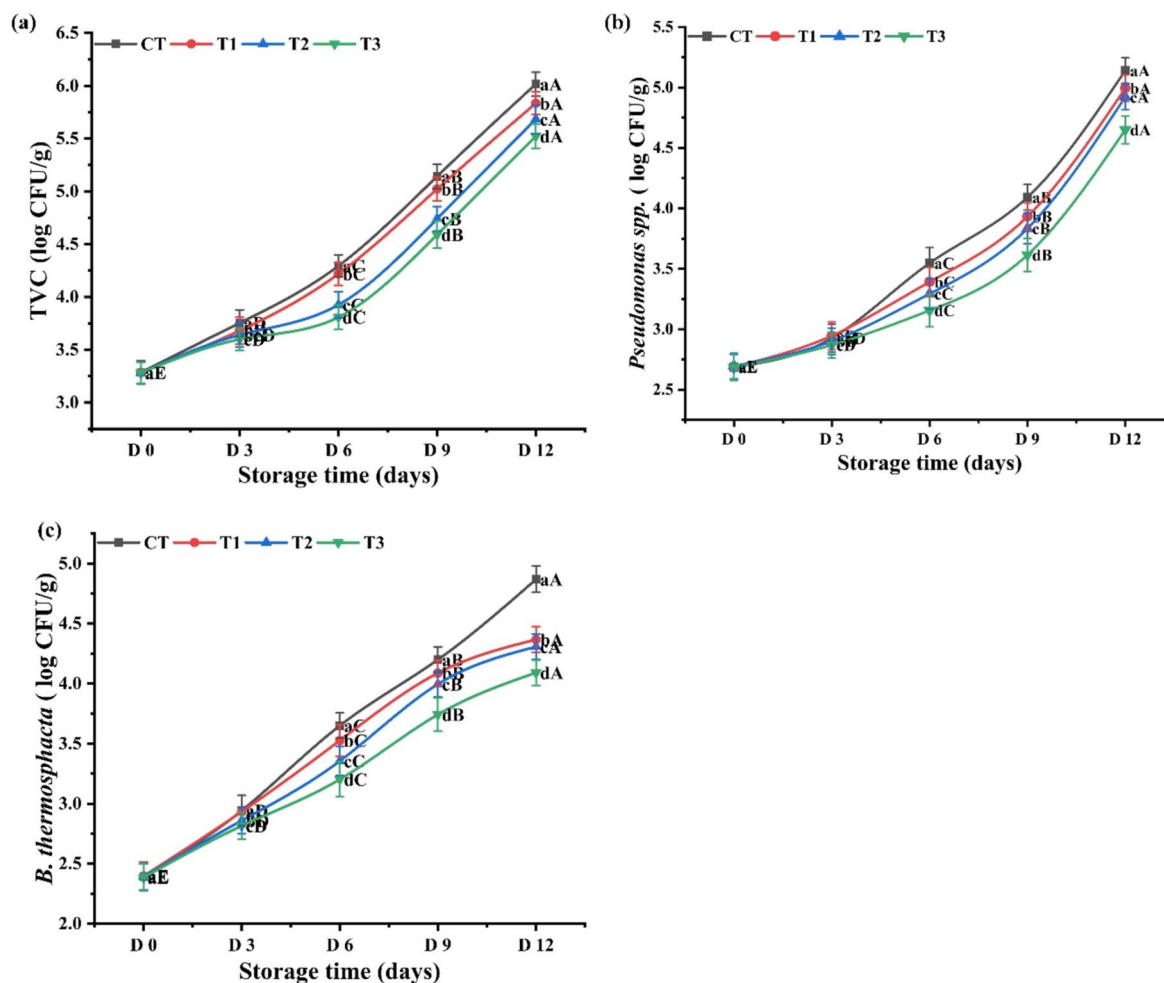


**Fig. 7** (a) Microbial analysis total viable count (TVC) (b) *Pseudomonas* spp. (c) *Brochothrix thermosphacta* results of packaged beef sausage slices during 12 d of refrigerated storage. Values are mean  $\pm$  SE ( $n=3$ ). <sup>a-c</sup> Means values are significantly different ( $p < 0.05$ ) across the treatments. While <sup>A-E</sup> means values are significantly different ( $p < 0.05$ ) across the storage duration. CT: Control (CG-CT (carboxymethyl cellulose and gum Arabic – control film)), T1 (Treatment 1): (CG-KPE1 ((carboxymethyl cellulose and gum Arabic – 1% of lyophilized kiwifruit peel powder extract film)), T2 (Treatment 2): (CG-KPE2 ((carboxymethyl cellulose and gum Arabic – 2% of lyophilized kiwifruit peel powder extract film)), and T3 (Treatment 3): (CG-KPE3 ((carboxymethyl cellulose and gum Arabic – 3% of lyophilized kiwifruit peel powder extract film))

Noipha (2012) reported a similar result trend among green tea extract based fabricated film application on TVC, yeasts and molds, and lactic acid bacteria in pork sausages for shelf-life extension studies.

### TBARS

Oxidation causes quality deterioration of meat products during processing and storage (Domínguez et al., 2021). Lipid oxidation decreases the nutritional value of meat products (Zhang, Xiao, & Ahn 2013; Zhao, et al., 2018) and packaging conditions influence product resistance to oxidation (Domínguez et al., 2021). Table 5 displayed higher TBARS values among CT samples during storage period. TBARS values indicated a significant difference

in CG-KPE film treatments compared to CT. This result could be linked to the high accumulation of lipid peroxides and hydroperoxides secondary products in CT treatments compared to the CG-KPE film treatments. The T1, T2, and T3 had a slightly lower TBARS values compared to CT samples, which could be ascribed to the stability of KPE polyphenol compounds (electron-repelling group). The results agree with the natural phenolic compounds of developed active packaged films that successfully stabilize the oxidative process in beef (Barbosa-Pereira et al., 2014). Also, the KPE antioxidant synergy reduced TBARS values by chelating ions among CG-KPE film treatments compared to CT relative to the increasing storage days.

**Table 5** The content of thiobarbituric acid reactive substances (TBARS)

Storage time (days)	TBARS (mg MDA/Kg)			
	CT	T1	T2	T3
D 0	0.14 ± 0.03 <sup>aC</sup>	0.11 ± 0.08 <sup>aC</sup>	0.08 ± 0.01 <sup>aE</sup>	0.07 ± 0.02 <sup>aD</sup>
D 3	0.23 ± 0.04 <sup>aC</sup>	0.22 ± 0.01 <sup>aC</sup>	0.18 ± 0.02 <sup>aD</sup>	0.16 ± 0.03 <sup>aD</sup>
D 6	0.48 ± 0.13 <sup>aBC</sup>	0.44 ± 0.04 <sup>aB</sup>	0.40 ± 0.05 <sup>aC</sup>	0.35 ± 0.06 <sup>aC</sup>
D 9	0.77 ± 0.26 <sup>aAB</sup>	0.76 ± 0.08 <sup>aA</sup>	0.65 ± 0.01 <sup>aB</sup>	0.60 ± 0.01 <sup>aB</sup>
D 12	0.96 ± 0.06 <sup>aA</sup>	0.90 ± 0.05 <sup>abA</sup>	0.80 ± 0.01 <sup>bcA</sup>	0.77 ± 0.01 <sup>cA</sup>

Values are mean ± SE (n=3)

<sup>a-c</sup> Means values are significantly different ( $p < 0.05$ ) across the treatments. Whiles <sup>A-E</sup> means values are significantly different ( $p < 0.05$ ) across the storage duration

CT Control (CG-CT (carboxymethyl cellulose and gum Arabic – control film)), T1 (Treatment 1): (CG-KPE1 (carboxymethyl cellulose and gum Arabic – 1% of lyophilized kiwifruit peel powder extract film)), T2 (Treatment 2): (CG-KPE2 (carboxymethyl cellulose and gum Arabic – 2% of lyophilized kiwifruit peel powder extract film)), and T3 (Treatment 3): (CG-KPE3 (carboxymethyl cellulose and gum Arabic – 3% of lyophilized kiwifruit peel powder extract film))

Cellulose excellent film formability (Roy & Rhim, 2020) and strong polymer interaction properties reduced chain reaction for an excellent oxygen species barrier (Umaraw et al., 2020). Therefore, KPE, together with cellulose enhanced the antioxidative effect of packaged beef sausage-slices to decline CG-KPE film treatments TBARS values compared to CT samples. Generally, CG-KPE packages exhibited a significant antioxidant capacity, good oxygen barrier to scavenge free radicals, and hydrogen donors to inhibit the oxidation process during storage for sausage shelf-life extension compared to CT samples. Alirezalu et al. (2021) reported a similar chelating ion and low oxygen permeance result of active film incorporated with  $\epsilon$ -polylysine application on the beef fillet. Lagos and Sobral (2019) reported the decline among beef hamburgers treated with chitosan–gelatin–boldo extract film stored at 4 °C. Apple-based edible coatings inhibited the lipid oxidation process among beef patties (Shin et al., 2017). Also, rosemary extract coated active film reduced packaged beef TBARS values (Barbosa-Pereira et al., 2014).

## Conclusion

Although the utilization of synthetic polymer in packaging materials provides desirable features such as preventing oxygen attack and chemical contamination, inhibiting deterioration, exerting enzymes activity to enhance tenderness, preventing UV light, and controlling color, aroma, and weight losses of processed meat products. However, environmental issues (pollution) are related to the use of non-biodegradable synthetic polymer-based packaging materials (disposable

problems) beyond the primary functions of protection and convenience. Therefore, KPE suitability as a biological material polysaccharides derivative research was needful to elucidate the functionalities of fabricated KPE active films for packaging application. In summary, the present study of CG-KPE composite films showed a decreased moisture content, swelling degree, and water solubility among physical properties. KPE induced CG-KPE composite film color and opacity to exhibit UV barrier properties. KPE polyphenolic compounds impacted CG-KPE film's antioxidant and antimicrobial ability on tested bacterial strains. Again, the thermal, mechanical, and morphological characterization indicated active packaging functionalities among CG-KPE films. As a natural polymeric matrix, CG-KPE films had an inherent quicker biodegradability feature. Consequently, studies on packaged sliced-beef sausage's pH and moisture content results revealed CG-KPE film impact on the physicochemical stability of products. Also, the CG-KPE film affected the packaged beef quality characteristics, revealed a better texture index, and exhibited more effective antimicrobial and antioxidant actions compared to CG-CT treatments during 12 d refrigerated storage. KPE could efficiently be used to fabricate active film packaging for beef sausage while exerting active packaging functionalities for products' shelf-life extension and quality in the meat sector.

## Acknowledgements

The authors wish to appreciate the Key Laboratory of Meat Processing and Quality Control, Ministry of Education China, Jiangsu Collaborative Innovation Center of Meat Production and Processing, Quality and Safety Control, College of Food Science and Technology, and Nanjing Agricultural University for the success of this study.

## Authors' contributions

EFB: Conceptualization, Methodology, Data Curation, Software, Writing Original Draft, Investigation, Validation. ZY: Methodology, Visualization, Investigation, Validation. JZ: Methodology, Visualization, Investigation, Validation. LZ: Methodology, Validation, Investigation, Visualization. LX: Visualization, Validation, Proofreading Manuscript. WZ: Supervision, Resources, Project administration, Revision, Editing, and Funding Acquisition.

## Funding

Not Applicable.

## Data availability

Not Applicable.

## Declarations

## Ethics approval and consent to participate

Not applicable.

## Consent for publication

Not applicable.

## Competing interests

Not applicable.

**Author details**

<sup>1</sup>Key Laboratory of Meat Processing and Quality Control, Ministry of Education China, Jiangsu Collaborative Innovation Center of Meat Production and Processing, Quality and Safety Control, College of Food Science and Technology, Nanjing Agricultural University, Nanjing 210095, Jiangsu, China.

Received: 27 October 2023 Accepted: 21 April 2024

Published online: 03 February 2025

**References**

- Akhtar, H. M. S., Riaz, A., Hamed, Y. S., Abdin, M., Chen, G., Wan, P., & Zeng, X. (2018). Production and characterization of CMC-based antioxidant and antimicrobial films enriched with chickpea hull polysaccharides. *International Journal of Biological Macromolecules*, *118*, 469–477. <https://doi.org/10.1016/j.ijbiomac.2018.06.090>
- Alirezalu, K., Pirouzi, S., Yaghoubi, M., Karimi-Dehkordi, M., Jafarzadeh, S., & Mousavi Khaneghah, A. (2021). Packaging of beef fillet with active chitosan film incorporated with  $\epsilon$ -polylysine: An assessment of quality indices and shelf life. *Meat Science*, *176*, 108475. <https://doi.org/10.1016/j.meatsci.2021.108475>
- Alnadari, F., Al-Dalali, S., Nasiru, M. M., Frimpong, E. B., Hu, Y., Abdalmegeed, D., Dai, Z., Abdulrahman, A. A., Chen, G., & Zeng, X. (2023a). A new natural drying method for food packaging and preservation using biopolymer-based dehydration film. *Food Chemistry*, *404*, 134689. <https://doi.org/10.1016/j.foodchem.2022.134689>
- Alnadari, F., Al-Dalali, S., Pan, F., Abdin, M., Frimpong, E. B., Dai, Z., Al-Dherasi, A., & Zeng, X. (2023b). Physicochemical characterization, molecular modeling, and applications of carboxymethyl chitosan-based multifunctional films combined with gum arabic and anthocyanins. *Food and Bioprocess Technology*, *16*, 2984–3002. <https://doi.org/10.1007/s11947-023-03122-0>
- Alnadari, F., Anthony, P. B., Abdin, M. A. S., Nasiru, M. M., Dai, Z., & Yuhang, H. X. Z. (2022). Development of hybrid film based on carboxymethyl chitosan-gum Arabic incorporated citric acid and polyphenols from Cinnamomum camphora seeds for active food packaging. *Journal of Polymers and the Environment*, *30*, 3582–3597. <https://doi.org/10.1007/s10924-021-02328-7>
- Arjenaki, N. O., Soltanzadeh, N., & Hamdami, N. (2019). Designing an active phase change material package for thermal and qualitative protection of meat. *Food Packaging and Shelf Life*, *21*, 100362. <https://doi.org/10.1016/j.foodpack.2019.100362>
- Arvanitoyannis, I. S., & Stratakos, A. C. (2012). Application of Modified Atmosphere Packaging and Active/Smart Technologies to Red Meat and Poultry: A Review. *Food and Bioprocess Technology*, *5*(5), 1423–1446. <https://doi.org/10.1007/s11947-012-0803-z>
- Barbosa-Pereira, L., Aurrekoetxea, G. P., Angulo, I., Paseiro-Losada, P., & Cruz, J. M. (2014). Development of new active packaging films coated with natural phenolic compounds to improve the oxidative stability of beef. *Meat Science*, *97*(2), 249–254. <https://doi.org/10.1016/j.meatsci.2014.02.006>
- Bassey, A. P., Chen, Y., Zhu, Z., Odeyemi, O. A., Frimpong, E. B., Ye, K., Li, C., & Zhou, G. (2021). Assessment of quality characteristics and bacterial community of modified atmosphere packaged chilled pork loins using 16S rRNA amplicon sequencing analysis. *Food Research International*, *145*, 110412. <https://doi.org/10.1016/j.foodres.2021.110412>
- Boateng, F. E., Yang, Z., & Zhang, W. (2022). Effects of kiwifruit peel extract and its antioxidant potential on the quality characteristics of beef sausage. *Antioxidants*, *11*(8), 1441. <https://doi.org/10.3390/antiox11081441>
- Cheng, S. Y., Wang, B. J., & Weng, Y. M. (2015). Antioxidant and antimicrobial edible zein/chitosan composite films fabricated by incorporation of phenolic compounds and dicarboxylic acids. *LWT - Food Science and Technology*, *63*(1), 115–121. <https://doi.org/10.1016/j.lwt.2015.03.030>
- da Costa, D. S., Costa, R. M. R., Takeuchi, K. P., & Lopes, A. S. (2023). Technological parameters of cassava starch/carboxymethyl cellulose blend-based films added of soy lecithin and tocopherol mix. *Polymer Testing*, *129*, 108245. <https://doi.org/10.1016/j.polymertesting.2023.108245>
- Deus, D., Kehrenberg, C., Schaudien, D., Klein, G., & Krischek, C. (2017). Effect of a nano-silver coating on the quality of fresh turkey meat during storage after modified atmosphere or vacuum packaging. *Poultry Science*, *96*(2), 449–457. <https://doi.org/10.3382/ps/pew308>
- Dias, M., Caleja, C., Pereira, C., Calheta, R. C., Kostic, M., Sokovic, M., Tavares, D., Baraldi, I. J., Barros, L., & Ferreira, I. C. F. R. (2020). Chemical composition and bioactive properties of byproducts from two different kiwi varieties. *Food Research International*, *127*, 108753. <https://doi.org/10.1016/j.foodres.2019.108753>
- Dominguez, R., Pateiro, M., Munekata, P. E., Zhang, W., Garcia-Oliveira, P., Carpena, Prieto, & M. A., Bohrer, B., & Lorenzo, J. M. (2021). Protein oxidation in muscle foods: A comprehensive review. *Antioxidants*, *11*(1), 60. <https://doi.org/10.3390/antiox11010060>
- Drago, E., Campardelli, R., Pettinato, M., & Perego, P. (2020). Innovations in Smart Packaging Concepts for Food: An Extensive Review. *Foods*, *9*(11), 1628. <https://doi.org/10.3390/foods9111628>
- Ebrahimzadeh, A., Pirzad, F., Tahanian, H., & Aghdam, M. S. (2019). Influence of gum Arabic enriched with GABA coating on oxidative damage of walnut kernels. *Food Technology and Biotechnology*, *57*(4), 554. <https://doi.org/10.17113/ftb.57.04.19.6380>
- Fu, Q. Q., Liu, R., Zhou, G. H., & Zhang, W. G. (2017). Effects of packaging methods on the color of beef muscles through influencing myoglobin status, metmyoglobin reductase activity and lipid oxidation. *Journal of Food Processing and Preservation*, *41*(1), 12740. <https://doi.org/10.1111/jfpp.12740>
- Gao, X., Zhang, W., & Zhou, G. (2014). Effects of glutinous rice flour on the physicochemical and sensory qualities of ground pork patties. *LWT - Food Science and Technology*, *58*(1), 135–141. <https://doi.org/10.1016/j.lwt.2014.02.044>
- Ghawanmeh, A. A., Tan, L. L., Ali, G. A., Assiri, M. A., & Chong, K. F. (2024). Optimization of carboxymethyl cellulose-gum Arab-based hydrogel beads for anticancer drugs delivery. *Journal of Molecular Liquids*, *393*, 123631. <https://doi.org/10.1016/j.molliq.2023.123631>
- Haddad, M. A., Dmour, H., Al-Khazaleh, J. M., Obeidat, M., Al-Abadi, A., Al-Shadaideh, A. N., & Al-mazra'awi, M. S., Shatnawi, M. A., & Iommi, C. (2020). Herbs and medicinal plants in Jordan. *Journal of AOAC International*, *103*(4), 925–929. <https://doi.org/10.1093/jaoacint/qs2026>
- Hafsa, J., Smach, M., & Ali, Ben Khedher, M. R., Charfeddine, B., Limes, K., Majdoub, H., & Rouatbi, S. (2016). Physical, antioxidant and antimicrobial properties of chitosan films containing Eucalyptus globulus essential oil. *LWT - Food Science and Technology*, *68*, 356–364. <https://doi.org/10.1016/j.lwt.2015.12.050>
- He, X., Fang, J., Chen, X., Zhao, Z., Li, Y., Meng, Y., & Huang, L. (2019). Actinidia chinensis Planch.: A review of chemistry and pharmacology. *Frontiers in Pharmacology*, *10*, 1236. <https://doi.org/10.3389/fphar.2019.01236>
- Kanatt, S. R., Rao, M. S., Chawla, S. P., & Sharma, A. (2013). Effects of chitosan coating on shelf-life of ready-to-cook meat products during chilled storage. *LWT - Food Science and Technology*, *53*(1), 321–326. <https://doi.org/10.1016/j.lwt.2013.01.019>
- Kang, S., Xiao, Y., Guo, X., Huang, A., & Xu, H. (2021). Development of gum arabic-based nanocomposite films reinforced with cellulose nanocrystals for strawberry preservation. *Food Chemistry*, *350*, 129199. <https://doi.org/10.1016/j.foodchem.2021.129199>
- Kang, S., Xiao, Y., Wang, K., Cui, M., Chen, D., Guan, D., Luan, G., & Xu, H. (2021). Development and evaluation of gum arabic-based antioxidant nanocomposite films incorporated with cellulose nanocrystals and fruit peel extracts. *Food Packaging and Shelf Life*, *30*, 100768. <https://doi.org/10.1016/j.foodpack.2021.100768>
- Katiyo, W., de Kock, H. L., Coorey, R., & Buys, E. M. (2020). Sensory implications of chicken meat spoilage in relation to microbial and physicochemical characteristics during refrigerated storage. *LWT*, *128*, 109468. <https://doi.org/10.1016/j.lwt.2020.109468>
- Kaya, M., Khadem, S., Cakmak, Y. S., Mujtaba, M., Ilk, S., Akyuz, L., Salaberria, A. M., Labidi, J., Abdulqadir, A. H., & Deligöz, E. (2018). Antioxidative and antimicrobial edible chitosan films blended with stem, leaf and seed extracts of Pistacia terebinthus for active food packaging. *RSC Advances*, *8*(8), 3941–3950. <https://doi.org/10.1039/C7RA12070B>
- Khedr, E. H. (2022). Application of different coating treatments to enhance storability and fruit quality of pomegranate (*Punica granatum* L., cv. Wonderful) during prolonged storage. *Revista Brasileira de Fruticultura*, *44*, e-855. <https://doi.org/10.1590/0100-29452022855>
- Kuchaiyaphum, P., Chotichayapong, C., Kajsanthia, K., & Saengsuwan, N. (2024). Carboxymethyl cellulose/poly (vinyl alcohol) based active film incorporated with tamarind seed coat waste extract for food packaging application. *International Journal of Biological Macromolecules*, *255*, 128203. <https://doi.org/10.1016/j.ijbiomac.2023.128203>

- Lagos, M. J. B., & Sobral, P. J. D. A. (2019). Application of active films with natural extract for beef hamburger preservation. *Ciência Rural*, 49(1), 1–9. <https://doi.org/10.1590/0103-8478cr20180797>
- Ma, T., Lan, T., Geng, T., Ju, Y., Cheng, G., Que, Z., Gao, G., Fang, Y., & Sun, X. (2019). Nutritional properties and biological activities of kiwifruit (*Actinidia*) and kiwifruit products under simulated gastrointestinal in vitro digestion. *Food & Nutrition Research*, 63 (0). <https://doi.org/10.29219/fnr.v63.1674>
- Mastromatteo, M., Gammariello, D., Costa, C., Lucera, A., Conte, A., and Del Nobile, M. A. (2014). Chilled storage of foods: Food packaging with antimicrobial properties. In C. A. Batt and P. Patel (Eds.), *Encyclopedia of food microbiology* (pp. 432–436). Cambridge: Academic Press. <https://doi.org/10.1016/B978-0-12-384730-0.00065-3>
- Muppalla, S. R., Kanatt, S. R., Chawla, S. P., & Sharma, A. (2014). Carboxymethyl cellulose–polyvinyl alcohol films with clove oil for active packaging of ground chicken meat. *Food Packaging and Shelf Life*, 2(2), 51–58. <https://doi.org/10.1016/j.foodpsl.2014.07.002>
- Nasiru, M. M., Boateng, E. F., Alnadari, F., Umair, M., Wang, Z., Senan, A. M., Yan, W., Zhuang, H., & Zhang, J. (2023). Dielectric barrier discharge cold atmospheric plasma treatment of egg white protein: Insights into the functional, rheological, and structural properties. *Food and Bioprocess Technology*, 1–22. <https://doi.org/10.1007/s11947-023-03159-1>
- Ozdemir, M., & Floros, J. D. (2004). Active food packaging technologies. *Critical Reviews in Food Science and Nutrition*, 44(3), 185–193. <https://doi.org/10.1080/10408690490441578>
- Pateiro, M., Domínguez, R., Bermúdez, R., Munekata, P. E., Zhang, W., Gagaoua, M., & Lorenzo, J. M. (2019). Antioxidant active packaging systems to extend the shelf life of sliced cooked ham. *Current Research in Food Science*, 1, 24–30. <https://doi.org/10.1016/j.crf.2019.10.002>
- Pereira de Abreu, D. A., Cruz, J. M., & Paseiro Losada, P. (2012). Active and intelligent packaging for the food industry. *Food Reviews International*, 28(2), 146–187. <https://doi.org/10.1080/87559129.2011.595022>
- Piñeros-Hernandez, D., Medina-Jaramillo, C., López-Córdoba, A., & Goyanes, S. (2017). Edible cassava starch films carrying rosemary antioxidant extracts for potential use as active food packaging. *Food Hydrocolloids*, 63, 488–495. <https://doi.org/10.1016/j.foodhyd.2016.09.034>
- Qin, Y., Liu, Y., Yong, H., Liu, J., Zhang, X., & Liu, J. (2019). Preparation and characterization of active and intelligent packaging films based on cassava starch and anthocyanins from *Lycium ruthenicum* Murr. *International Journal of Biological Macromolecules*, 134, 80–90. <https://doi.org/10.1016/j.ijbiomac.2019.05.029>
- Qin, Y., Liu, Y., Zhang, X., & Liu, J. (2020). Development of active and intelligent packaging by incorporating betalains from red pitaya (*Hylocereus polyrhizus*) peel into starch/polyvinyl alcohol films. *Food Hydrocolloids*, 100, 105410. <https://doi.org/10.1016/j.foodhyd.2019.105410>
- Riaz, A., Lagnika, C., Luo, H., Dai, Z., Nie, M., Hashim, M. M., Liu, C., Song, J., & Li, D. (2020). Chitosan-based biodegradable active food packaging film containing Chinese chive (*Allium tuberosum*) root extract for food application. *International Journal of Biological Macromolecules*, 150, 595–604. <https://doi.org/10.1016/j.ijbiomac.2020.02.078>
- Roy, S., & Rhim, J. W. (2020). Carboxymethyl cellulose-based antioxidant and antimicrobial active packaging film incorporated with curcumin and zinc oxide. *International Journal of Biological Macromolecules*, 148, 666–676. <https://doi.org/10.1016/j.ijbiomac.2020.01.204>
- Salehi, F., Inanloodoghrou, M., & Karami, M. (2023). Rheological properties of carboxymethyl cellulose (CMC) solution: Impact of high intensity ultrasound. *Ultrasonics Sonochemistry*, 101, 106655. <https://doi.org/10.1016/j.ultsonch.2023.106655>
- Sariyel, V., Aygun, A., Coklar, H., Narinc, D., & Akbulut, M. (2022). Effects of prestorage application of gum arabic coating on the quality of table eggs during storage. *Kafkas Üniversitesi Veteriner Fakültesi Dergisi*, 28(3). <https://doi.org/10.9775/kvfd.2022.27077>
- Shang, X., Jiang, H., Wang, Q., Liu, P., & Xie, F. (2019). Cellulose-starch hybrid films plasticized by aqueous ZnCl<sub>2</sub> solution. *International Journal of Molecular Sciences*, 20(3), 474. <https://doi.org/10.3390/ijms20030474>
- Shin, S. H., Chang, Y., Lacroix, M., & Han, J. (2017). Control of microbial growth and lipid oxidation on beef product using an apple peel-based edible coating treatment. *LWT*, 84, 183–188. <https://doi.org/10.1016/j.lwt.2017.05.054>
- Sims, I. M., & Monro, J. A. (2013). Fiber: Composition, structures, and functional properties. In M. Boland & P. J. Moughan (Eds.), *Advances in food and nutrition research* (pp. 81–99). Cambridge: Academic Press. <https://doi.org/10.1016/B978-0-12-394294-4.00005-5>
- Siripatrawan, U., & Noipha, S. (2012). Active film from chitosan incorporating green tea extract for shelf life extension of pork sausages. *Food Hydrocolloids*, 27(1), 102–108. <https://doi.org/10.1016/j.foodhyd.2011.08.011>
- Suriyatem, R., Auras, R. A., & Rachtanapun, P. (2018). Improvement of mechanical properties and thermal stability of biodegradable rice starch-based films blended with carboxymethyl chitosan. *Industrial Crops and Products*, 122, 37–48. <https://doi.org/10.1016/j.indcrop.2018.05.047>
- Tan, Z., Yi, Y., Wang, H., Zhou, W., Yang, Y., & Wang, C. (2016). Physical and Degradable Properties of Mulching Films Prepared from Natural Fibers and Biodegradable Polymers. *Applied Sciences*, 6(5), 147. <https://doi.org/10.3390/app6050147>
- Tiamiyu, Q. O., Adebayo, S. E., & Yusuf, A. A. (2023). Gum Arabic edible coating and its application in preservation of fresh fruits and vegetables: A review. *Food Chemistry Advances*, 100251. <https://doi.org/10.1016/j.focha.2023.100251>
- Tyagi, V., & Thakur, A. (2023). Applications of biodegradable carboxymethyl cellulose-based composites. *Results in Materials*, 100481, 100481. <https://doi.org/10.1016/j.rinma.2023.100481>
- Umaraw, P., Munekata, P. E. S., Verma, A. K., Barba, F. J., Singh, V. P., Kumar, P., & Lorenzo, J. M. (2020). Edible films/coating with tailored properties for active packaging of meat, fish and derived products. *Trends in Food Science & Technology*, 98, 10–24. <https://doi.org/10.1016/j.tifs.2020.01.032>
- Venkatesan, J., Hur, W., Gupta, P. K., Son, S. E., Lee, H. B., Lee, S. J., Ha, C. H., Cheon, S. H., & Seong, G. H. (2023). Gum Arabic-mediated liquid exfoliation of transition metal dichalcogenides as photothermic anti-breast cancer candidates. *International Journal of Biological Macromolecules*, 244, 124982. <https://doi.org/10.1016/j.ijbiomac.2023.124982>
- Volf, I., Ignat, I., Neamtu, M., & Popa, V. (2014). Thermal stability, antioxidant activity, and photo-oxidation of natural polyphenols. *Chemical Papers*, 68(1), 121–129. <https://doi.org/10.2478/s11696-013-0417-6>
- Wang, L., Guo, H., Wang, J., Jiang, G., Du, F., & Liu, X. (2019). Effects of Herba Lophatheri extract on the physicochemical properties and biological activities of the chitosan film. *International Journal of Biological Macromolecules*, 133, 51–57. <https://doi.org/10.1016/j.ijbiomac.2019.04.067>
- Wang, S., Qiu, Y., & Zhu, F. (2021). Kiwifruit (*Actinidia* spp.): A review of chemical diversity and biological activities. *Food Chemistry*, 350, 128469. <https://doi.org/10.1016/j.foodchem.2020.128469>
- Wang, S., Xia, P., Wang, S., Liang, J., Sun, Y., Yue, P., & Gao, X. (2019). Packaging films formulated with gelatin and anthocyanins nanocomplexes: Physical properties, antioxidant activity and its application for olive oil protection. *Food Hydrocolloids*, 96, 617–624. <https://doi.org/10.1016/j.foodhyd.2019.06.004>
- Wojdyło, A., Nowicka, P., Oszmiński, J., & Golis, T. (2017). Phytochemical compounds and biological effects of *Actinidia* fruits. *Journal of Functional Foods*, 30, 194–202. <https://doi.org/10.1016/j.jff.2017.01.018>
- Wu, J., Zhong, F., Li, Y., Shoemaker, C. F., & Xia, W. (2013). Preparation and characterization of pullulan–chitosan and pullulan–carboxymethyl chitosan blended films. *Food Hydrocolloids*, 30(1), 82–91. <https://doi.org/10.1016/j.foodhyd.2012.04.002>
- Xu, T., Gao, C., Feng, X., Yang, Y., Shen, X., & Tang, X. (2019). Structure, physical and antioxidant properties of chitosan–gum arabic edible films incorporated with cinnamon essential oil. *International Journal of Biological Macromolecules*, 134, 230–236. <https://doi.org/10.1016/j.ijbiomac.2019.04.189>
- Yang, W., Xie, Y., Jin, J., Liu, H., & Zhang, H. (2019). Development and application of an active plastic multilayer film by coating a plantaricin bm-1 for chilled meat preservation. *Journal of Food Science*, 84(7), 1864–1870. <https://doi.org/10.1111/1750-3841.14608>
- Ye, M., Neetoo, H., & Chen, H. (2008). Control of *Listeria monocytogenes* on ham steaks by antimicrobials incorporated into chitosan-coated plastic films. *Food Microbiology*, 25(2), 260–268. <https://doi.org/10.1016/j.fm.2007.10.014>
- Zamuz, S., Munekata, P. E., Dzuvoor, C. K., Zhang, W., Sant'Ana, A. S., & Lorenzo, J. M. (2021). The role of phenolic compounds against *Listeria monocytogenes* in food. A review. *Trends in Food Science & Technology*, 110, 385–392.
- Zhang, J., Zhang, W., Zhou, L., & Zhang, R. (2021). Study on the influences of ultrasound on the flavor profile of unsmoked bacon and its underlying metabolic mechanism by using HS-GC-IMS. *Ultrasonics Sonochemistry*, 80, 105807. <https://doi.org/10.1016/j.ultsonch.2021.105807>

- Zhang, J., Zhang, Y., Wang, Y., Xing, L., & Zhang, W. (2020). Influences of ultrasonic-assisted frying on the flavor characteristics of fried meatballs. *Innovative Food Science & Emerging Technologies*, 62(March), 102365. <https://doi.org/10.1016/j.ifset.2020.102365>
- Zhang, W., Xiao, S., & Ahn, D. U. (2013). Protein oxidation: Basic principles and implications for meat quality. *Critical reviews in food science and nutrition*, 53(11), 1191–1201. <https://doi.org/10.1080/10408398.2011.577540>
- Zhang, W., Xiao, S., Samaraweera, H., Lee, E. J., & Ahn, D. U. (2010). Improving functional value of meat products. *Meat Science*, 86(1), 15–31. <https://doi.org/10.1016/j.meatsci.2010.04.018>
- Zhao, Y., Hou, Q., Cao, S., Wang, Y., Zhou, G., & Zhang, W. (2019). Effect of regenerated cellulose fiber on the properties and microstructure of emulsion model system from meat batters. *Food Hydrocolloids*, 87, 83–89. <https://doi.org/10.1016/j.foodhyd.2018.07.044>
- Zhao, Y., Hou, Q., Zhuang, X., Wang, Y., Zhou, G., & Zhang, W. (2018). Effect of regenerated cellulose fiber on the physicochemical properties and sensory characteristics of fat-reduced emulsified sausage. *LWT*, 97, 157–163. <https://doi.org/10.1016/j.lwt.2018.06.053>
- Zhao, Y., Zhou, S., Xia, X., Tan, M., Lv, Y., Cheng, Y., Tao, Y., Lu, J., & Du, J., & Wang, H. (2022). High-performance carboxymethyl cellulose-based hydrogel film for food packaging and preservation system. *International Journal of Biological Macromolecules*, 223, 1126–1137. <https://doi.org/10.1016/j.ijbio mac.2022.11.102>

### Publisher's Note

Springer Nature remains neutral with regard to jurisdictional claims in published maps and institutional affiliations.